Medical Science, Osakagas Group Welfare Foundation, Osaka Kidney Foundation, Japan, Preventive Arteriosclerosis Research Association, and Kurozumi Medical Foundation. We would like to express our deepest gratitude to the following people for their continuous support of our population survey in this area: Dr Otosaburo Hishikawa (president), Dr Katsuyuki Kawanishi (committee member in chief for the city health checkup service), and other members of Suita City Medical Association, and Shigeru Kobayashi, director of the City Health Center. We would also like to express our greatest thanks to the members of our attendants' society (Satsuki-Junyu-kai) for their cooperation and assistance in our survey on risk factors and preventive activity on cardiovascular diseases. We are also deeply grateful to Dr Soichiro Kitamura, president of the National Cardiovascular Center, for consideration of our research.

References

1. Mazza A, Giugliano D, Motti C, Cortese C, Andreotti F, Marra G, Nulli A. Glycemia, MTHFR genotype and low homocysteine in uncomplicated type 2 diabetic patients. *Atherosclerosis*. 2000;149:223–224.
2. Stampfer MJ, Malinow MR, Willett WC, Newcomer LM, Upson B, Ullmann D, Tishler PV, Hennekens CH. A prospective study of plasma homocyst(e)ine and risk of myocardial infarction in US physicians. *JAMA*. 1992;268:877–881.
3. Selhub J, Jacques PF, Bostom AG, D Agostino RB, Wilson PW, Belanger AJ, O Leary DH, Wolf PA, Schaefer EJ, Rosenberg IH. Association between plasma homocysteine concentrations and extracranial carotid-artery stenosis. *N Engl J Med*. 1995;332:286–291.
4. McCully KS. Homocysteine and vascular disease. *Nat Med*. 1996;2: 386–389.
5. Refsum H, Ueland PM, Nygard O, Vollset SE. Homocysteine and cardiovascular disease. *Ann Rev Med*. 1998;49:31–62.
6. Frosst P, Blom HJ, Milos R, Goyette P, Sheppard CA, Matthews RG, Boers GJ, den Heijer M, Kluijtmans LA, van den Heuvel LP. A candidate genetic risk factor for vascular disease: a common mutation in methylenetetrahydrofolate reductase. *Nat Genet*. 1995;10:111–113.
7. Ma J, Stampfer MJ, Hennekens CH, Frosst P, Selhub J, Horsford J, Malinow MR, Willett WC, Rozen R. Methylenetetrahydrofolate reductase polymorphism, plasma folate, homocysteine, and risk of myocardial infarction in US physicians. *Circulation*. 1996;94:2410–2416.
8. Kluijtmans LA, Kastelein JJ, Lindemans J, Boers GH, Heil SG, Bruschke AV, Jukema JW, van den Heuvel LP, Trijbels FJ, Boerma GJ, Verheugt FW, Willems F, Blom HJ. Thermolabile methylenetetrahydrofolate reductase in coronary artery disease. *Circulation*. 1997;96:2573–2577.
9. Morita H, Kurihara H, Tsubaki S, Sugiyama T, Hamada C, Kurihara Y, Shindo T, Oh Hashi Y, Kitamura K, Yazaki Y. Methylenetetrahydrofolate reductase gene polymorphism and ischemic stroke in Japanese. *Arterioscler Thromb Vasc Biol*. 1998;18:1465–1469.
10. Salomon O, Steinberg DM, Zivelin A, Gitel S, Dardik R, Rosenberg N, Berliner S, Inbal A, Many A, Lubetsky A, et al. Single and combined prothrombotic factors in patients with idiopathic venous thromboembolism: prevalence and risk assessment. *Arterioscler Thromb Vasc Biol*. 1999;19:511–518.
11. Beaudry M, Spence JD. Measurement of atherosclerosis: development of an atherosclerosis severity index. *Clin Exp Hypertens*. 1989;11:943–956.
12. Reed DM, Resch JA, Hayashi T, MacLean C, Yano K. A prospective study of cerebral artery atherosclerosis. *Stroke*. 1988;19:820–825.
13. Sutton Tyrrell K, Bostom A, Selhub J, Zeigler Johnson C. High homocysteine levels are independently related to isolated systolic hypertension in older adults. *Circulation*. 1997;96:1745–1749.
14. Wilcken DE, Wang XL, Sim AS, McCredie RM. Distribution in healthy and coronary populations of the methylenetetrahydrofolate reductase (MTHFR) C677T mutation. *Arterioscler Thromb Vasc Biol*. 1996;16: 878–882.
15. Deloughery TG, Evans A, Sadeghi A, McWilliams J, Henner WD, Taylor LM, Press RD. Common mutation in methylenetetrahydrofolate reductase: correlation with homocysteine metabolism and late-onset vascular disease. *Circulation*. 1996;94:3074–3078.
16. Mannami T, Konishi M, Baba S, Nishi N, Terao A. Prevalence of asymptomatic carotid atherosclerotic lesions detected by high-resolution ultrasonography and its relation to cardiovascular risk factors in the general population of a Japanese city: the Suita study. *Stroke*. 1997;28: 518–525.
17. Baba T, Tanaka H, Date C, Hayashi M, Tanaka Y, Okazaki K, Nakamura M, Iida M, Komachi Y, Yoshikawa K, et al. The standardization of measurement of lipids for epidemiologic study of stroke. *Jpn J Hyg*. 1983;38:606–613.
18. Fortin LJ, Genest J. Measurement of homocyst(e)ine in the prediction of arteriosclerosis. *Clin Biochem*. 1995;28:155–162.
19. Witte JS. Gene-environment interaction. In: Elston R, Olson J, Palmer L, eds. *Biostatistical Genetics and Genetic Epidemiology*. Cleveland, Ohio: John Wiley & Sons; 2002:297–299.
20. Clarke R, Daly L, Robinson K, Naughten E, Cahalane S, Fowler B, Graham I. Hyperhomocysteinemia: an independent risk factor for vascular disease. *N Engl J Med*. 1991;324:1149–1155.
21. Gallagher PM, Meleady R, Shields DC, Tan KS, McMaster D, Rozen R, Evans A, Graham IM, Whitehead AS. Homocysteine and risk of premature coronary heart disease: evidence for a common gene mutation. *Circulation*. 1996;94:2154–2158.
22. de Franchis R, Mancini FP, D Angelo A, Sebastio G, Fermo I, de Stefano V, Margaglione M, Mazzola G, di Minno G, Andria G. Elevated total plasma homocysteine and 677C→T mutation of the 5, 10-methylenetetrahydrofolate reductase gene in thrombotic vascular disease. *Am J Hum Genet*. 1996;59:262–264.
23. Hwang SJ, Beaty TH, Liang KY, Coresh J, Khoury MJ. Minimum sample size estimation to detect gene-environment interaction in case-control designs. *Am J Epidemiol*. 1994;140:1029–1037.
24. Guttormsen AB, Ueland PM, Nesthus I, Nygard O, Schneede J, Vollset SE, Refsum H. Determinants and vitamin responsiveness of intermediate hyperhomocysteinemia (> or = 40 micromol/liter): the Hordaland Homocysteine Study. *J Clin Invest*. 1996;98:2174–2183.
25. Harmon DL, Woodside JV, Yarnell JW, McMaster D, Young IS, McCrum EE, Gey KF, Whitehead AS, Evans AE. The common "thermolabile" variant of methylene tetrahydrofolate reductase is a major determinant of mild hyperhomocysteinemia. *QJM*. 1996;89:571–577.
26. Jacques PF, Bostom AG, Williams RR, Ellison RC, Eckfeldt JH, Rosenberg IH, Selhub J, Rozen R. Relation between folate status, a common mutation in methylenetetrahydrofolate reductase, and plasma homocysteine concentrations. *Circulation*. 1996;93:7–9.
27. Demuth K, Atger V, Borderie D, Benoit MO, Sauvaget D, Lotersztajn S, Moatti N. Homocysteine decreases endothelin-1 production by cultured human endothelial cells. *Eur J Biochem*. 1999;263:367–376.
28. Ross R. The pathogenesis of atherosclerosis: a perspective for the 1990s. *Nature*. 1993;362:801–809.
29. Wu Y, Tomon M, Sumino K. Methylenetetrahydrofolate reductase gene polymorphism and ischemic stroke: sex difference in Japanese. *Kobe J Med Sci*. 2001;47:255–262.
30. Passaro A, Vanini A, Calzoni F, Alberti L, Zamboni PF, Fellin R, Solini A. Plasma homocysteine, methylenetetrahydrofolate reductase mutation and carotid damage in elderly healthy women. *Atherosclerosis*. 2001;157:175–180.
31. Motti C, Gnasso A, Bernardini S, Massoud R, Pastore A, Rampa P, Federici G, Cortese C. Common mutation in methylenetetrahydrofolate reductase: correlation with homocysteine and other risk factors for vascular disease. *Atherosclerosis*. 1998;139:377–383.
32. Dierkes J, Jeckel A, Ambrosch A, Westphal S, Luley C, Boeing H. Factors explaining the difference of total homocysteine between men and women in the European Investigation Into Cancer and Nutrition Potsdam Study. *Metabolism*. 2001;50:640–645.
33. Schwartz SM, Siscovick DS, Malinow MR, Rosendaal FR, Beverly RK, Hess DL, Psaty BM, Longstreth WT, Koepsell TD, Raghunathan TE, Reitsma PH. Myocardial infarction in young women in relation to plasma total homocysteine, folate, and a common variant in the methylenetetrahydrofolate reductase gene. *Circulation*. 1997;96:412–417.
34. van Bockxmeer FM, Mamotte CD, Vasikaran SD, Taylor RR. Methylenetetrahydrofolate reductase gene and coronary artery disease. *Circulation*. 1997;95:21–23.
35. Selhub J, Jacques PF, Wilson PW, Rush D, Rosenberg IH. Vitamin status and intake as primary determinants of homocysteinemia in an elderly population. *JAMA*. 1993;270:2693–2698.
36. Lwin H, Yokoyama T, Date C, Yoshiike N, Kokubo Y, Tanaka H. Are the associations between life-style related factors and plasma total homocysteine concentration different according to polymorphism of 5, 10-methylenetetrahydrofolate reductase gene (C677T MTHFR)? A cross-sectional study in a Japanese rural population. *J Epidemiol*. 2002;12:126–135.
37. Nygard O, Vollset SE, Refsum H, Stensvold I, Tverdal A, Nordrehaug JE, Ueland M, Kvale G. Total plasma homocysteine and cardiovascular risk profile: The Hordaland Homocysteine Study. *JAMA*. 1995;274: 1526–1533.

Journal of Human Hypertension (2004) 18, 693–699

www.nature.com/jhh

ORIGINAL ARTICLE

Losartan, an angiotensin II (AT_1) receptor antagonist, preserves cerebral blood flow in hypertensive patients with a history of stroke

H Moriwaki[1], H Uno[1], Y Nagakane[1], K Hayashida[2], K Miyashita[1] and H Naritomi[1]
[1]*Department of Cerebrovascular Medicine, National Cardiovascular Center, Suita, Osaka, Japan;*
[2]*Department of Radiology, National Cardiovascular Center, Suita, Osaka, Japan*

In patients with severe hypertension, chronic heart failure or a history of stroke, the lower limit of autoregulation of cerebral blood flow (CBF) is shifted to higher levels of blood pressure (BP) than those observed in healthy subjects. The aim of pharmacotherapy for hypertensive patients with an impaired autoregulation of CBF should be to reduce BP while preserving an appropriate CBF. In the present study, 16 hypertensive patients who had had an episode of stroke more than 4 weeks previously were administered the angiotensin II (AT_1) receptor antagonist losartan at daily doses of 25–100 mg for 4 weeks. Systolic and diastolic blood pressures were recorded for 24 h using an ambulatory BP monitoring system. CBF in both hemispheres of the cerebrum and cerebellum was quantified using single photon emission tomography with *N*-isopropyl-*p*-[^{123}I]iodoamphetamine. At baseline, CBF was 29.7±6.7 ml/min/100 g in the cerebrum and 31.5±7.5 ml/min/100 g in the cerebellum. At the end of treatment, BP was lower, while CBF increased by 7.7% in the cerebrum, and remained at the baseline level in the cerebellum. Thus, CBF was preserved despite the reduction in BP. We consider the use of losartan is advantageous for hypertensive patients with a history of stroke in whom autoregulation of CBF is potentially impaired.
Journal of Human Hypertension (2004) **18**, 693–699. doi:10.1038/sj.jhh.1001735
Published online 6 May 2004

Keywords: stroke; cerebral blood flow; angiotensin; losartan; hypertension

Introduction

It is well known that cerebral blood flow (CBF) in healthy subjects is autoregulated to maintain a stable flow rate within a wide range of changes in blood pressure (BP), with the lower limit of mean BP being as low as 50–60 mmHg. However, in patients with severe hypertension, CBF is affected when the mean BP decreases below 100 mmHg.[1] Furthermore, in patients with a cerebrovascular disease, the autoregulation of CBF may be disturbed so that the lower limit necessary to maintain a constant CBF is shifted to a BP level higher than that seen in healthy subjects.[2,3] This impaired autoregulation is considered to be mostly a consequence of structural damage of small arteries in the brain, accompanying with higher susceptibility to vasoactive substances.

Correspondence: Dr H Moriwaki, Department of Cerebrovascular Medicine, National Cardiovascular Center, 5-7-1, Fujishirodai, Suita, Osaka 565-8565, Japan. E-mail: hmoriwa@hsp.ncvc.go.jp
Received 26 May 2003; revised 11 November 2003; accepted 17 November 2003; published online 6 May 2004

On the basis of knowledge of the actions of angiotensin II on vascular beds in organs including the brain, therapeutic benefits of intervention of the renin–angiotensin system has been considered to normalize the lower limit of CBF autoregulation in patients with an impaired cerebral circulation. The ACE inhibitor captopril was the first drug to maintain CBF while BP was reduced beyond lower limit of autoregulation in hypertensive rats.[4,5] Similar results were obtained in patients with chronic heart failure.[6,7] In 1992, Kuriyama *et al*[8] reported that the ACE inhibitor enalapril preserved CBF in hypertensive patients with an old history of stroke with effectively reducing BP, indicating successful shifting of the lower limit of CBF autoregulation to lower BP levels. These findings led us to postulate that a direct blockade of angiotensin II receptors may result in a reduction of BP while maintaining an appropriate CBF in patients whose autoregulation is impaired.

In the present study, we assessed the effect of the angiotensin II (AT_1) receptor antagonist (AIIA) losartan on CBF in hypertensive patients with a

history of stroke. We used an ambulatory BP monitoring (ABPM) system to measure BP, and single photon emission computed tomography (SPECT) with the tracer *N*-isopropyl-*p*-[^{123}I]iodoamphetamine to measure the blood flow in both hemispheres of the cerebrum and cerebellum.

Patients and methods

Study patients

In-patients and outpatients of either gender, ⩾20–<75 years old, who had hypertension and a history of stroke were eligible for the study, provided they satisfied the following criteria during a pretreatment screening period of 2 days–one week.

(a) Hypertensive patients. That is, their systolic BP (SBP) and diastolic BP (DBP) in the supine position measured using a mercury sphygmomanometer, at least twice on their visits to the hospital, were ⩾140 or ⩾90 mmHg, respectively, and average 24 h ambulatory SBP (24-h SBP) during the screening period was ⩾135 mmHg or their average 24 h DBP (24-h DBP) was ⩾85 mmHg.
(b) Patients with a chronic cerebrovascular disease. That is, the patients who had had an episode of stroke (cerebral infarction, defined by X-ray computed tomography or magnetic resonance imaging), more than 4 weeks, previously.

The principal investigator decided the eligibility of the patients. Exclusion criteria were as follows:

(a) Severe hypertension (DBP⩾110 mmHg).
(b) Secondary hypertension.
(c) Patients who could not discontinue antihypertensive drug therapy.
(d) A serum creatinine concentration of ⩾2.5 mg/dl.
(e) Patients with a severe cerebrovascular lesion.
(f) Patients showing hypersensitivity to the test drug.
(g) Patients of pregnancy, possibility of pregnancy, and in a period of lactation.
(h) Patients suffering from a severe hepatic disease.

Study design

The overview of the study design is shown in Figure 1. This study was designed as a self-control study by comparing values of BP and CBF on weeks 2 and 4 of treatment to those observed during the screening period (baseline) in each patient. Before the screening period, a washout period of at least 2 weeks was required for the patients who had been treated with antihypertensive drugs. Following the screening period, the patients were administered losartan once daily at the starting dose of 25 mg. However, in cases in which a patient's compliance was judged by investigator(s) to be sufficiently good for the administration of a higher dose, a starting

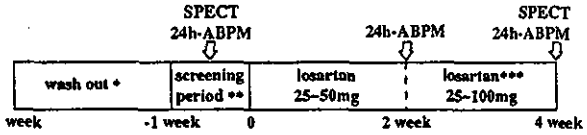

Figure 1 Study design for treatment of hypertensive patients with a history of stroke. *Patients who had been treated with any antihypertensive drug were entered after a washout period of at least 2 weeks. **Two-day to 1-week screening period was followed by the treatment period of 4 weeks. CBF was measured by SPECT and mean 24-h BP by ABPM during the screening period, and the last days of weeks 2 and 4. ***When BP control was inadequate within the first 2 weeks (see Study design), the dose of losartan was escalated.

dose of 50 mg was applied. Thus, in the first 2 weeks the dose of losartan was 25 or 50 mg. In the following 2 weeks, however, the dose was escalated if the 24-h SBP/DBP of <135/85 mmHg was not achieved, or if reductions in 24-h SBP of ⩾10 mmHg and 24-h DBP of ⩾5 mmHg were not satisfied.

BP was recorded by ABPM and CBF was measured by SPECT during the screening period, and at weeks 2 and 4 of treatment. To measure 24-h BP, the patients were fitted with an ABPM and the pressure was recorded every 30 min from 0600 to 2200 (daytime) and every 60 min from 2200 to 0600 (nighttime). For measurements of the 24-h BP, the ABPM device Type TM-2421(A&D Co. Ltd., Tokyo, Japan) was used. CBF was evaluated using the *N*-isopropyl-*p*-[^{123}I]iodoamphetamine (^{123}I-IMP) autoradiographic method based on a two-compartment kinetic model in which the input function is determined by arterial counting 10 min after the injection of ^{123}I-IMP instead of frequent blood sampling. The absolute value was obtained by the table look-up method after the arterial count was converted to the scale of the SPECT count using a cross calibration factor that was determined *a priori* in a phantom study.[9,10]

SPECT was performed using a ring-type gamma camera (Headtome SET-070; Shimadzu, Kyoto, Japan) with an 8-mm FWHM obtained. Patients were immobilized with eyes covered, and 4.5 mCi (166.5 MBq) of ^{123}I-IMP was injected intravenously. Data collection began 15 min after injection of the tracer. Image data over 30-min were collected onto a 128 × 128 matrix using a general all-purpose collimator. All data were corrected for an attenuation of 0.1/cm and tomographic data were reconstructed using a filtered back-projection algorithm. The regions of interest (ROIs) were drawn on the both sides of middle cerebral artery territories and cerebellar hemispheres according to our previous report.[11] These ROIs were defined with reference to the atlas of Kretschmann and Weinrich.[12] If an infarct was included within a standard ROI, the size of the ROI was reduced to avoid the area of infarct.

The study protocol was in accordance with the declaration of Helsinki and was reviewed and approved by the Institutional Review Board of the

National Cardiovascular Center. Written informed consent was obtained from all enrolled patients.

Statistics

All values are expressed as the mean ± s.d. Differences of values on weeks 2 and 4 from the respective baseline values were analysed by one-sample *t*-test. Differences with a *P*-value of <0.05 were considered statistically significant.

Results

Patient characteristics at baseline and at week 4

We enrolled 16 patients in the study. One patient showed increases in AST (GOT) and γ-GTP at the week-2 determination point and the principal investigator considered it was desirable for this patient to discontinue the treatment. Changes of CBF were therefore assessed in 15 patients. Table 1 summarizes baseline characteristics of the 15 patients and their CBF measured at baseline, and CBF measured at week 4 as the result. Averaged values are, age: 63.8 ± 6.2-year-old, office SBP/DBP: 158.7 ± 11.4/84.9 ± 9.5 mmHg, 24-h SBP/DBP: 154.1 ± 14.1/90.2 ± 9.8 mmHg, CBF at baseline (cerebrum/cerebellum): 29.7 ± 6.7/31.5 ± 7.5 ml/min/100 g.

Blood pressure

Figure 2 shows changes in BP measured using the ABPM system during treatment with losartan. Both 24-h SBP and 24-h DBP decreased significantly during treatment (SBP: from 154.1 ± 14.1 at baseline to 140.3 ± 19.6 on week 4 ($P<0.05$); DBP: from 90.2 ± 9.8 at baseline to 82.1 ± 12.2 on week 4 ($P<0.05$)). The difference in BP between daytime and nighttime increased but it did not reach statistical significance during the study period (day/night; SBP: 157.3 ± 13.5/147.8 ± 18.0 mmHg, DBP: 91.8 ± 9.8/87.3 ± 11.2 mmHg at baseline; SBP: 145.7 ± 19.7/129.5 ± 20.8 mmHg, DBP: 84.5 ± 12.2/77.3 ± 13.3 mmHg on week 4), suggesting that the diurnal BP change tended to be restored to some extent during the treatment (Figure 2). In stratified analyses of the effect of losartan in 15 patients, a successful reduction in 24-h SBP and 24-h DBP (SBP: from 150.4 ± 16.8 at baseline to 126.5 ± 13.7 mmHg, on week 4, DBP: from 86.8 ± 9.2 at baseline to 73.3 ± 5.1 mmHg, on week 4) was observed in eight patients, while in seven patients, 24-h SBP and 24-h DBP decreased only slightly without statistical significance (SBP: from 158.3 ± 9.9 at baseline to 156.1 ± 11.3 mmHg, on week 4, DBP: from 94.1 ± 9.7 at baseline to 92.1 ± 9.7 mmHg, on week 4).

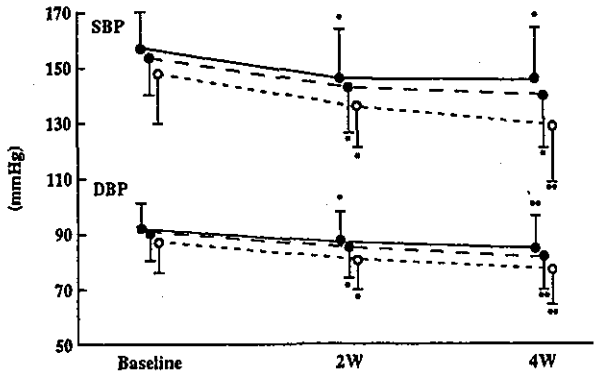

Figure 2 Changes in BP in hypertensive patients with a history of stroke. Patients were treated with losartan at doses of 25–100 mg/day during 4 weeks. A circle with a bar represents the mean value ± s.d ($n=15$). *$P<0.05$, **$P<0.01$ *vs* baseline. –●–, daytime average; ···○···, nighttime average; ----●----, 24-h average.

Cerebral blood flow

Types of cerebrovascular disease (CVD) of our patients were atherothrombotic brain infarction (ATBI), lacunar infarction (LA), cardioembolic infarction (CE), and aortogenic infarction (Aorta). There were three patients who had periventricular hyperintensity (PVH). There was no specific trend in response to losartan in relation to CVD types. CBF values of individual patients measured at week 4 are summarized in Table 1.

Figure 3 shows global blood flow in the cerebrum and cerebellum, at baseline and after 4 weeks of treatment with losartan. The average blood flow in the cerebrum increased by 7.7% (from 29.7 ± 6.7 to 32.0 ± 8.0 ml/min/100 g) with statistical significance ($P<0.05$), while in the cerebellum the blood flow remained unchanged (from 31.5 ± 7.5 to 33.4 ± 8.7 ml/min/100 g; NS).

We next divided the patients into two subgroups based on their responsiveness of BP to losartan. The upper panels of Figure 4 show the change in CBF in the cerebellum and cerebrum of the eight patients who showed an effective decrease of 24-h SBP and 24-h DBP (subgroup A). In this subgroup the increase in CBF in the cerebrum was statistically significant. The lower panels of Figure 4 show the CBF in the cerebellum and cerebrum of the seven patients in whom no decrease of 24-h SBP and 24-h DBP was observed (subgroup B). CBF did not increase and remained unchanged, although two patients in this subgroup showed prominent increases; one from 35.8 to 43.1 (20.4%) and the other from 40.0 to 50.5 ml/min/100 g (26.3%) in the cerebellum, and from 34.4 to 42.4 (23.3%) and 38.2 to 49.9 (30.6%) in the cerebrum, respectively.

Serum uric acid and safety evaluation

Laboratory measurements revealed a statistically significant decrease in serum uric acid in all

Table 1 Patient characteristics and CBF at baseline and at week 4

Patient number	Gender	Age (years)	Weeks after the event of stroke	Previous anti-hypertensive therapy	BP (mmHg) systolic/diastolic		Dipper (D), Extreme dipper (ED) or Non dipper (N)	CVD					CBF (ml/min/100 g) cerebrum/cerebellum	
					Office BP	24-h BP		CVD type	MRA findings	Lesion location	Lesion size (cm^3)	Modified Rankin scale	Baseline	Week 4
1	M	71	140.6	Yes	158/77	142/93	N	ATBI	Lt SCA.O Rt MCA. 70% St	Lt Cerebellum	3.0	1	21.7/22.5	22.5/24.4
2	M	66	53.1	Yes	177/85	169/79	N	ATBI	Rt PCA. wall irregular	Rt Occipital	12.0	1	29.9/28.6	29.0/27.6
3	M	72	5.0	Yes	151/74	139/75	D	ATBI	Lt ICA 70% St	Lt frontal	1.0	0	24.6/25.4	28.4/28.8
4	M	64	4.1	Yes	169/103	157/90	N	LA	n.p.	Lt corona radiata	1.4	0	24.5/28.4	26.2/29.8
5	M	53	4.4	Yes	148/87	132/91	N	CE	n.p.	Rt MCA area	71.7	2	21.7/22.5	22.3/22.4
6	M	70	671.3	No	162/82	177/105	N	ATBI	Rt MCA. branch.O	Rt MCA area	30.0	2	20.6/22.0	26.3/26.4
7	F	60	254.9	Yes	152/82	162/87	N	ATBI	Lt MCA 50% St	Lt corona radiata	1.6	0	34.4/35.8	42.4/43.1
8	M	71	5.3	Yes	161/85	157/84	N	ATBI	BA. 90% St	Lt pons	1.5	3	26.8/25.2	25.9/24.4
9	M	69	69.6	No	143/86	129/87	N	LA	n.p.	Rt corona radiata	1.2	1	37.0/43.7	39.1/42.0
10	M	62	5.7	Yes	156/80	148/90	D	LA	n.p.	Lt thalamus	0.8	0	34.8/36.2	32.6/36.0
11	F	53	5.9	Yes	161/91	169/90	N	Aorta	Rt VA 50% St	Rt pons	0.5	0	42.4/42.4	39.6/39.3
12	M	58	6.7	No	164/79	129/81	ED	Aorta	n.p.	Lt frontal	13.9	1	31.4/34.0	35.1/38.9
13	M	61	5.0	Yes	158/93	149/105	N	LA	n.p.	Lt corona radiata	0.8	0	32.3/38.2	35.1/41.6
14	M	65	4.6	Yes	140/68	155/86	D	ATBI	BA. 70% St	Lt Cerebellum	3.0	1	25.5/27.3	25.9/26.3
15	F	61	5.3	Yes	181/102	171/110	N	LA	n.p.	Lt corona radiata	0.5	0	38.2/40.0	49.9/50.5

Abbreviations: ATBI = atherothrombotic brain infarction; LA = lacunar *infarction*; CE = cardioembolic infarction; Aorta = aortogenic embolic infarction; Lt = left; Rt = right; ICA = internal carotid artery; MCA = middle cerebral artery; PCA = posterior cerebral artery; SCA = superior cerebellar artery; O = occlusion; *St* = stenosis; BA = basilar artery; VA = vertebral artery; n.p. = no particular.

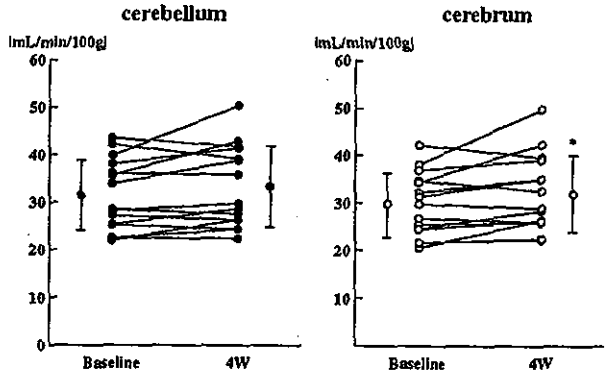

Figure 3 Changes in individual CBF in the cerebrum and cerebellum in hypertensive patients with a history of stroke. The blood flow is expressed as ml/min/100 g brain ($n=15$). A circle with a bar represents the mean value ±s.d. The increase in CBF observed in the cerebrum was statistically significant (*$P<0.05$ *vs* baseline).

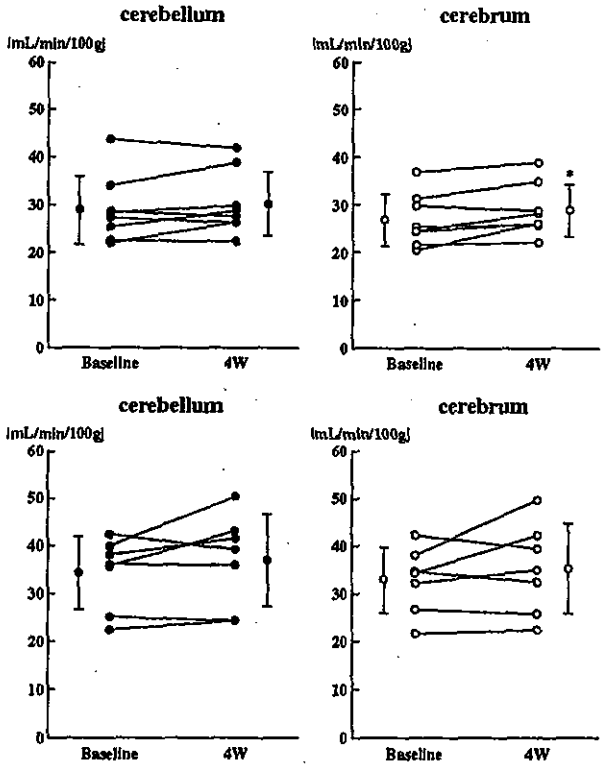

Figure 4 Changes in CBF in patients divided according to the response of BPs to losartan during the 4-week treatment. Upper panels correspond to subgroup A (BP was reduced; $n=8$) and the lower panels to subgroup B (BP was not reduced; $n=7$). A circle with a bar represents the mean value ±s.d. In subgroup A, the increase in CBF was statistically significant in the cerebrum (*$P<0.05$ *vs* baseline).

patients: the average concentration of serum uric acid was 356.9±49.2 μmol/l at baseline and 312.5±56.5 μmol/l at week 4 (12% reduction, $P<0.01$). As for adverse effects, six patients reported experiences that were considered by the investigator to be possibly or probably related to the study treatment. The patient who was dropped out of the study showed an increase in AST (GOT) from 51 to 72 IU/l and of γ-GTP from 296 to 380 IU/l and vomiting in the first 2-weeks of losartan treatment. In another patient, slight increases in AST (GOT) from 30 to 65 IU/l and ALT (GPT) from 24 to 69 IU/l and γ-GTP from 215 to 348 IU/l were observed. In four other patients, dizziness, transient loss of consciousness, diarrhea and swelling and tenderness of the right hand were reported. No severe or fatal adverse events were observed during the 4 weeks of treatment with losartan.

Discussion

In our present study, treatment of hypertensive patients with a history of stroke for 4 weeks with losartan resulted in an effective average reduction of 13.7 mmHg in 24-h SBP and of 8.1 mmHg in 24-h DBP, as measured using an ABPM system. Whereas, the average blood flow in the cerebrum showed a statistically significant increase. The average blood flow in the cerebellum tended to increase, but the increase did not reach statistical significance. Thus, the blood flow in both cerebrum and cerebellum was well preserved, despite the decrease of BP. However, there were seven patients who showed only a 2.1 mmHg decrease in 24-h SBP, and a 2.0 mmHg decrease in 24-h DBP. As a result, of a total of 15 patients, eight were well responded and seven were poorly responded to losartan. Although there was no statistical correlation between the change in BP and the change in CBF, in patients whose BPs were reduced, only one had a reduced flow in the cerebrum, while in patients whose BPs were poorly reduced, three had the reduced flow (Figure 4). These results led us to postulate that the more effectively losartan reduces BP, the more favourably CBF is preserved.

In our patients the average baseline CBF, excluding the area of infarct, was 29.7±6.7 ml/min/100 g in the cerebrum and 31.5±7.5 ml/min/100 g in the cerebellum. Kuriyama *et al*[8] reported that global CBF in patients with a history of stroke and impaired autoregulation was 42.3±6.1 ml/min/100 g. Iida *et al*[10] reported CBF was 39.0±2.9 ml/min/100 g in the cerebellum of healthy volunteers. By comparison, the CBF of our patients was low, indicating an impaired cerebral circulation.

The beneficial effect of ACE inhibition on CBF was first reported by Barry *et al*[4] and Jarden *et al*[5] in hypertensive rats, using captopril. They demonstrated that although BP fell below the previously established lower limit of autoregulation, CBF remained unchanged. Clinical evidences of this

effect of ACE inhibitors was obtained in patients with chronic heart failure,[6,7] and then in hypertensive patients with a history of stroke.[8] Our present results are consistent with such previous findings, thereby the effect of ACE inhibitors to preserve CBF is probably attributed to the interference of angiotensin II AT_1 receptor mediated actions, since losartan is a selective angiotensin II AT_1 receptor antagonist (AIIA). The important role of angotensin II AT1 receptors to affect CBF is also supported by the results reported by Nishimura *et al*,[13] who demonstrated the effect of the AIIA candesartan to preserve CBF in spontaneously hypertensive rats with cerebral ischaemia. Furthermore, the effect of repeated administration of losartan may differ from that of ACE inhibitors. Recent advances in interventional pharmacology of the renin–angiotensin system have revealed clear differences between the properties of AIIAs and those of ACE inhibitors. First, AIIAs inhibit angiotensin II AT_1 receptors, but not AT_2 receptors which may counteract the actions of AT_1 receptors.[14] The actions of AT_2 are considered to include vasodilation, induction of apoptosis, interference of vascular remodeling, all which may contribute to preserve the vascular structure.[15] However, ACE inhibitors cannot block the production of angiotensin II via a non-ACE enzyme, such as chymase, which is known to exist in the vascular tissue.[16,17]

Taken together, the beneficial effect of losartan in hypertensive patients with a history of stroke may be explained by its acute effect that is similar to that of ACE inhibitors, as well as by its chronic effect on vascular tissue, through which it ameliorates its structure and function. If the latter were the case, it is considered that the effects of a blockade of angiotensin II AT_1 receptors by losartan are amelioration of the damaged vascular structure and restoration of a physiologically normal tone in resistant arteries; thereby the lower limit of autoregulation would be reset to a level of BP lower than that established as a consequence of stroke. These assumptions must be substantially demonstrated in the future in both experimental and clinical studies.

Recently, an interesting clinical study involving hypertensive patients with left ventricular hypertrophy, named LIFE study, was reported.[18] In this study, 4588 patients were treated with the beta-blocker atenolol and 4605 patients with the AIIA losartan, for more than 60 months. The efficacy of these drugs regarding BP reduction was similar. However, the proportion of patients with first event of stroke was significantly lower in the losartan group than in the atenolol group. The investigators of this mega-trial did not state the reason for this difference, but it may be possible that losartan reduced the risk of infarction by protecting cerebral vessels from structural changes. If this were the case, the result of our present study would be compatible with the result of the LIFE study in terms of protection of function and structure of vascular beds in the brain.

In conclusion, administration of losartan to hypertensive patients with a history of stroke for four consecutive weeks resulted in a decrease of BP with a preserved blood flow in both the cerebrum and cerebellum. The blockade of angiotensin II AT_1 receptors by losartan is considered to be safe in such patients, because it preserves the function of autoregulation of cerebral blood flow in therapy of BP control.

References

1 Strandgaard S, Olesen J, Skinhoj E, Lassen NA. Autoregulation of brain circulation in severe arterial hypertension. *BMJ* 1973; 1: 507–510.
2 Kuriyama Y *et al*. Report of six cases of hemodynamic TIA and its casual relations among hemodynamic parameters. *Jpn J Stroke* 1987; 9: 463–468.
3 Kuriyama Y, Sawada T, Omae T. Antihypertensive drugs and cerebral circulation. In: Omae T, Zanchetti A (ed). *How Should Elderly Hypertensive Patients be Treated?* Springer: Tokyo, 1989, pp 69–81.
4 Barry DI *et al*. Cerebrovascular aspects of converting-enzyme inhibition I: effects of intravenous captopril in spontaneously hypertensive and normotensive rats. *J Hypertens* 1984; 2: 589–597.
5 Jarden JO *et al*. Cerebrovascular aspects of converting-enzyme inhibition II: blood–brain barrier permeability and effect of intracerebroventricular administration of captopril. *J Hypertens* 1984; 2: 599–604.
6 Rajagopalan B, Raine AEG, Cooper R, Ledingham JGG. Changes in cerebral blood flow in patients with severe congestive cardiac failure before and after captopril treatment. *Am J Med* 1984; 76(5B): 86–90.
7 Paulson OB *et al*. Effect of captopril on the cerebral circulation in chronic heart failure. *Eur J Clinical Invest* 1986; 16: 124–132.
8 Kuriyama Y, Nakamura M, Sawada T, Omae T. Normalization of cerebral blood flow autoregulation after administration of a converting enzyme inhibitor (enalapril) in old stroke patients with hypertension. *High Blood Pressure* 1992; 1: 239–244.
9 Iida H *et al*. Quantitative mapping of regional cerebral blood flow using iodine-123-IMP and SPECT. *J Nucl Med* 1994; 35: 2019–2030.
10 Iida H *et al*. A multicenter validation of regional cerebral blood flow quantitation using [^{123}I]iodoamphetamine and single photon emission computed tomography. *J Cereb Blood Flow Metab* 1996; 16: 781–793.
11 Moriwaki H *et al*. Iodine-123-iomazenil and iodine-123-iodoamphetamine SPECT in major cerebral artery occlusive disease. *J Nucl Med* 1998; 39: 1348–1353.
12 Kretschmann HJ, Weinrich W. *Neuroanatomy and Cranial Computed Tomography*. Thieme: New York, 1986, pp 70–74.
13 Nishimura Y, Ito T, Saavedra JM. Angiotensin II AT1 blockade normalizes cerebrovascular autoregulation and reduces cerebral ischemia in spontaneously hypertensive rats. *Stroke* 2000; 31: 2478–2486.

14 Chung O, Unger T. Angiotensin II receptor blockade and end-organ protection. *Am J Hypertens* 1999; **12**: 150S–156S.
15 Horiuchi M, Akishita M, Dzau VJ. Recent progress in angiotensin II type 2 receptor research in the cardiovascular system. *Hypertension* 1999; **33**: 613–621.
16 Husain A. The chymase–angiotensin system in humans. *J Hypertens* 1993; **11**: 1155–1159.
17 Takai S, Jin D, Sakaguchi M, Miyazaki M. Chymase-dependent angiotensin II formation in human vascular tissue. *Circulation* 1999; **100**: 654–658.
18 Dahlöf B *et al*, for the LIFE Study Group. Cardiovascular morbidity and mortality in the losartan intervention for endpoint reduction in hypertension study (LIFE): a randomized trial against atenolol. *Lancet* 2002; **359**: 995–1003.

Vertebral Artery Occlusion in Duplex Color-Coded Ultrasonography

Kozue Saito, MD; Kazumi Kimura, MD; Kazuyuki Nagatsuka, MD; Keiko Nagano, MD; Kazuo Minematsu, MD; Satoshi Ueno, MD; Hiroaki Naritomi, MD

Background and Purpose—To establish the diagnostic criteria for the site of occlusion in the vertebral arteries (VAs) using duplex color-coded ultrasonography.

Methods—In 128 consecutive patients who underwent conventional cerebral angiography, we prospectively measured the diameter, mean flow velocity (MV), peak systolic flow velocity, and end-diastolic flow velocity of both VAs. The diameter-ratio (diameter of contralateral VA divided by that of target VA) and MV-ratio (MV of contralateral VA divided by that of target VA) were determined. Based on the angiographic findings, we classified the VAs into 4 types (5 groups) as follows: (1) the origin of VA occlusion (Origin group: n=9); (2) VA occlusion before branching into the posterior inferior cerebellar artery (PICA) (Before group: n=10); (3A) symptomatic VA occlusion after branching into the PICA (After group: n=12); (3B) asymptomatic or hypoplastic occlusive VA after branching into the PICA (PICA end group: n=15); and (4) no significant occlusive lesions in the VA (Control group: n=194).

Results—No flow signals in the VAs apparently indicated the Origin group. Preserved peak systolic flow velocity but end-diastolic flow velocity of zero cm/s indicated the Before group. MV <18 cm/s and MV-ratio ≥1.4 indicated the PICA end group or After group. Furthermore, these groups could be distinguished as follows: a diameter-ratio <1.4 indicated the After group. A diameter-ratio ≥1.4 indicated the PICA end group. Either MV ≥18 cm/s or MV <18 cm/s in combination with MV-ratio <1.4 indicated the Control group.

Conclusion—Duplex color-coded ultrasonography can accurately diagnose the site of VA occlusion. (***Stroke.* 2004;35: 1068-1072.)**

Key Words: vertebral artery ■ occlusion ■ ultrasonography ■ ultrasonography, Doppler, duplex ■ diagnosis ■ vertebrobasilar circulation

Duplex color-coded ultrasonography is useful in the evaluation of occlusive lesions in the carotid[1–6] and vertebral[7–13] arteries (VAs) in acute stroke patients. The diagnostic criteria for occlusive lesions in the carotid arteries have been already established.[1,5] Duplex color-coded ultrasonography is also valuable to evaluate pathological VAs, such as VA occlusion,[13,14] subclavian steal phenomenon,[12,15–17] and vertebral arterial dissection.[18–21] The site of VA occlusions is divided into 3 groups: VA origin occlusions, VA occlusions before branching into the posterior inferior cerebellar artery (PICA), and VA occlusions after branching into the PICA. However, the diagnostic criteria in duplex ultrasonography for the site of VA occlusion remain unclear. Furthermore, a few VAs show asymptomatic occlusion or naturally hypoplastic VA ending at the PICA (PICA end).[22] The aim of the present study was to establish the criteria for determining the site of occlusion of VAs, including VAs ending at the PICA, using duplex color-coded ultrasonography.

Methods

We prospectively assessed the 256 VAs of 128 consecutive patients (91 men and 37 women, mean±SD; 63.4±12.2 years) admitted to the National Cardiovascular Center and who underwent intraarterial digital subtraction angiography (IA-DSA) between May 1, 2003 and July 31, 2003. We excluded 16 VAs with 50% to 99% stenosis in diameter on angiography because the flow velocity was also affected by the stenotic lesions. Therefore, 240 VAs were examined in the present study. Eighty-four patients had acute cerebral infarctions (33 in the vertebrobasilar circulation and 51 in the internal carotid arterial circulation), 12 had transient ischemic attacks, 20 had old infarctions (12 in the vertebrobasilar circulation, 8 in the internal carotid arterial circulation), 3 had cerebral hemorrhages, and the remaining 9 nonstroke patients had asymptomatic arterial stenotic or occlusive lesions (1 in the basilar artery, 2 in the middle cerebral artery, and 6 in the internal carotid artery). Eighty-four patients with acute stroke underwent IA-DSA within 2.6±3.9 days of stroke onset. Informed consent for IA-DSA was obtained from both the patient and family.

Selective IA-DSA was performed using a biplane, high-resolution angiography system (Angio Rex Super-G and DFP-2000A; Toshiba) with a matrix of 1024×1024 pixels. A catheter was inserted into the right brachial artery or femoral artery in accordance with the

Received December 27, 2003; accepted January 30, 2004.

From Cerebrovascular Division (K.S., K.K., K.Nagatsuka, K.Nagano, K.M., H.N.), Department of Medicine, National Cardiovascular Center, Japan; Department of Neurology (S.U.), Nara Medical University, Japan.

Correspondence to Dr Kozue Saito, Fujishirodai, Suita, Osaka 565-8565, Japan. E-mail ksaito@hsp.ncvc.go.jp

Stroke is available at http://www.strokeaha.org

DOI: 10.1161/01.STR.0000125857.63427.59

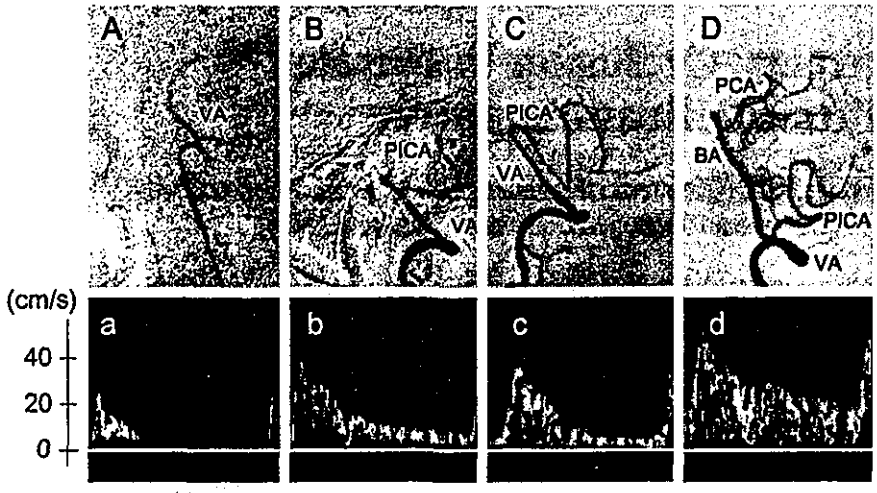

Figure 1. Angiogram (lateral view of vertebral arterial angiography) and Doppler waveforms of patients in the Before group (A and a), After group (B and b), PICA end group (C and c), and Control group (D and d). A and a, The VA was occluded before branching into the PICA. The Doppler waveform showed no EDV. B and b, The VA was occluded after branching into the PICA. The Doppler waveform showed EDV and MV was lower than those of the Control group. C and c, The VA ended in the PICA and did not continue to the union of the BA. The Doppler waveform also showed EDV and MV were lower than those of the Control group. D and d, No significant occlusion of the VA. The Doppler waveform showed EDV and MV was highest among all groups. VA indicates vertebral artery; BA, basilar artery; PICA, posterior inferior cerebellar artery; PCA, posterior cerebral artery.

Seldinger method, and then guided to the cerebral arteries for diagnostic 4-vessel angiography. Based on the angiographic findings, we classified the VA vessels into 4 types (5 groups) as follows: (1) the origin of VA occlusion (Origin group); (2) VA occlusion before branching into the PICA (Before group); (3) VA occlusion after branching into the PICA, which was divided into 2 groups—(3A) VA symptomatic occlusion after branching into the PICA (After group) and (3B) hypoplastic or asymptomatic occlusive VA after branching into the PICA (PICA end group); and (4) no significant occlusive lesions in the VAs (Control group). The After group was defined as symptomatic VA occlusion associated with acute ischemic stroke presented as a new infarct on MRI including diffusion-weighted imaging (DWI) or transient ischemic attack (TIA) in the vertebrobasilar circulation. The clinical diagnosis of stroke and TIA was made by the attendant physician from the result of MRI (DWI) and neurological findings. When VA occlusion was symptomatic, we identified it as the After group, even if the diameter of the target VA was smaller than that of the contralateral VA.

Using B-mode scans with color imaging and pulsed-Doppler, one investigator with no previous knowledge of the patients' clinical information including angiographic findings (K.S.) measured the flow velocities of both VAs within 48 hours before or after IA-DSA. We used a Sonos 5500 duplex color-coded ultrasonographic device (Philips) equipped with a 7.5-MHz transducer. First, we measured the diameter of the both VAs at the C3–4, C4–5, or C5–6 levels. Second, the flow velocities of the VAs were obtained between the transverse process at the C3–4, C4–5, or C5–6 levels of the cervical spine. The sample volume (2 to 3 mm, depending on the diameter of the VA) was set within the VAs and flow velocities were measured, taking care to maintain an adequate angle of ≤60 degrees between the beam and the VAs. The pulse repetition frequency was 3.0 or 3.5 Hz, and the low pass filter was set at 70 Hz. We obtained the peak systolic flow velocity (PSV), the end-diastolic flow velocity (EDV), and the time-averaged peak mean flow velocity (MV), corrected using the adequate angle for both VAs. Resistance index (RI) was defined as (PSV-EDV)÷PSV. The diameter-ratio (diameter of contralateral VA divided by diameter of target VA) and MV-ratio (MV of contralateral VA divided by that of target VA) were also determined. The diameter, diameter-ratio, and flow velocity data for each group were expressed as mean±SD.

Brain computed tomography (CT) and MRI including DWI were performed in all the patients to assess new brain infarctions. Conventional MRI T1-weighted (repetition time [TR]/echo time [TE]; 630/14), T2-weighted (TR/TE; 5400/99), and fluid-attenuation inversion recovery (FLAIR) (TR/TE; 9000/105) images were obtained. DWI was performed simultaneously using a spin-echo planar imaging sequence. Diffusion gradients were applied in the x, y, and z directions, with a b value of 1000/cm^2.

Statistical analysis was performed using the Mann-Whitney U test and Kruskal-Wallis test. A value of $P<0.05$ was accepted as indicating statistical significance. Sensitivity and specificity curves were produced to obtain the best cut-off value for each diagnostic criterion.

Results

The VAs were clearly displayed in all patients using B-mode with color imaging, and blood flow velocity was successfully evaluated by pulse Doppler (Figure 1). Table 1 shows the VA diameter, diameter-ratio, MV, MV-ratio, EDV, and RI of each VA.

Origin Group

Although the VAs were clearly detected using B-mode with color imaging, no blood flow signals, including MV and

TABLE 1. Parameters in Each Group

Group	N of Vessels	VA Diameter (mm)	Diameter-ratio	MV (cm/s)	MV-ratio	EDV (cm/s)	RI
Control	194	3.76±0.66	0.97±0.27	25.26±7.54	0.94±0.37	15.10±5.39	0.66±0.09
Origin	9	3.25±1.08	1.39±0.31	0	—	0	—
Before	10	3.25±0.72	1.20±0.42	7.24±4.64	2.38±1.55	0	1
After	12	3.37±0.64	1.10±0.23	12.92±3.29	2.00±0.80	6.69±3.74	0.78±0.14
PICA end	15	2.62±0.39	1.68±0.31	13.95±3.22	2.31±1.73	7.09±2.46	0.76±0.09
Total	240						

Diameter-ratio indicates diameter of contralateral VA divided by that of target VA; MV, mean flow velocity; MV-ratio, mean flow velocity of contralateral VA divided by that of target VA; EDV, end-diastolic flow velocity; RI, resistance index=(peak systolic flow velocity−end-diastolic flow velocity)÷peak systolic flow velocity.

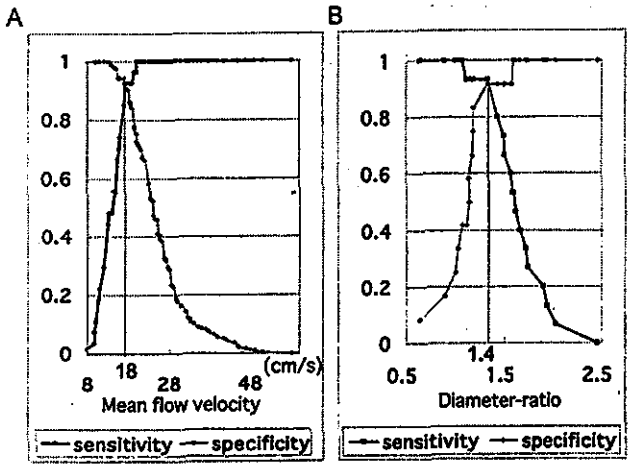

Figure 2. A, Sensitivity and specificity curve analysis for MV to discriminate the After and PICA-end groups from the Control group. B, Sensitivity and specificity curve analysis for diameter-ratio to discriminate the PICA end group from the After group.

EDV, in the VAs could be detected using pulse Doppler, allowing the Origin group VAs to be easily identified.

Before Group

Peak systolic flow velocity was preserved, but EDV was zero cm/s in all patients in the Before group. In addition, the MV (7.2±4.6 cm/s) was the lowest among all the groups, excluding the Origin group ($P<0.0001$). Excluding the Origin group, an EDV of zero cm/s allowed the Before group VAs to be easily distinguished from the other groups.

Distinguishing After and PICA End Groups From the Control Group

Of the 3 groups other than the Origin and Before groups, the MV, EDV, and RI of the After and PICA end groups (After group:12.9±3.3 cm/s, 6.7±3.7 cm/s, 0.78±0.14, respectively; PICA end group:14.0±3.2 cm/s, 7.1±2.5 cm/s, 0.76±0.09, respectively) were lower than those of the Control group (25.3±7.5 cm/s, 15.1±5.4 cm/s, 0.66±0.09, respectively) ($P<0.0001$). Using sensitivity–specificity curve analysis for discriminating the Control group from the After and PICA end group, the cut-off point of the RI and MV were 0.7 (sensitivity 74.0% and specificity 72.6%) and 18 cm/s (sensitivity 92.6% and specificity 90.2%; Figure 2A), respectively. Therefore, MV was a better parameter than RI for discriminating the After and PICA end groups from the Control group. However, 18 of 43 patients with MV <18 cm/s belonged to the Control group and the positive predictive value was low (58.1%). Of these 43 VAs with MV <18 cm/s, the sensitivity–specificity curve for MV-ratio to distinguish the After and PICA end groups from the Control group showed a cut-off value of 1.4 and gave a sensitivity of 84.0% and specificity of 82.3%. If we used the combined criteria of both MV <18 cm/s and MV-ratio ≥1.4 to distinguish the After and PICA end groups from the Control group, then sensitivity, specificity, accuracy, and positive predictive value were 85.2%, 97.4%, 95.9%, and 82.1%, respectively.

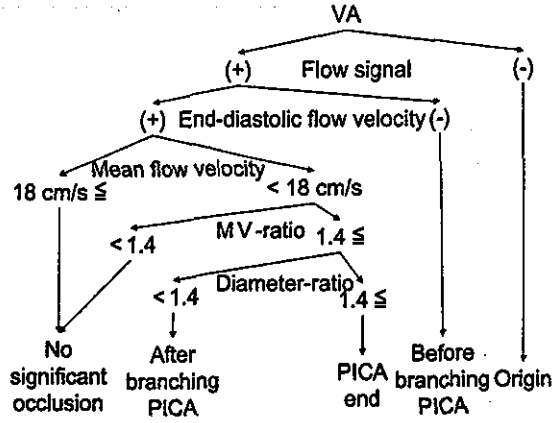

Figure 3. Ultrasonographic diagnostic algorithm for the site of VA occlusion.

Distinguishing the PICA End Group From the After Group

No significant difference in MV, EDV, and RI between the After group and PICA end group was observed. However, the diameter (2.62±0.39 mm) in the PICA end group was the smallest among all the groups (Before group: 3.25±0.72 mm; After group: 3.37±0.64 mm; Control group: 3.76±0.66 mm) ($P<0.0001$). The diameter-ratio (1.68±0.31) in the PICA end group was also the largest among all the groups (Before group: 1.20±0.42; After group: 1.10±0.23; Control group: 0.97±0.27, respectively) ($P<0.0001$). Using sensitivity–specificity curve analysis for discriminating the PICA end group from the After group, the cut-off point of VA diameter and diameter-ratio were 2.8 mm (sensitivity 73.3% and specificity 83.3%) and 1.4 (sensitivity 93.3% and specificity 91.7%), respectively (Figure 2B). Therefore, the diameter-ratio was a better parameter than VA diameter for discriminating the PICA end group from the After group.

Ultrasonographic Diagnostic Criteria

Figure 3 shows the criteria for the site of VA occlusion, including PICA end with duplex color-coded ultrasonography based on the present results. Table 2 shows the relationship between the cerebral angiographic findings and our ultrasonographic diagnosis. One VA vessel of the After group had the diameter-ratio ≥1.4. Therefore, we classified it as the PICA end, based on ultrasonographic criteria. The accuracy for conformity between them was 95.0%.

Discussion

The present study has established the ultrasonographic diagnostic criteria for determining the site of VA occlusion. Kimura et al[14] demonstrated the usefulness of measurement of VA flow velocity using duplex ultrasonography for the localization of the site of VA occlusion. They reported EDV of zero cm/s in a VA occlusion sited before branching into the PICA, which is consistent with the present findings. Furthermore, they described that the MV was significantly lower in a VA occlusion after branching into the PICA than in the nonocclusive VA group. However, accurate diagnostic criteria for differentiating these types were not established in their study.

TABLE 2. Comparison of Angiographic and Ultrasonographic Diagnoses

		Ultrasonographic Diagnosis					
		Control	Origin	Before	After	PICA End	Total
Angiographic Diagnosis	Control	189	0	0	3	2	194
	Origin	0	9	0	0	0	9
	Before	0	0	10	0	0	10
	After	2	0	0	9	1	12
	PICA end	2	0	1	1	11	15
	Total	193	9	11	13	14	240

In the present study, except for patients in the Origin and Before groups, 98.9% of patients with MV ≥18 cm/s had nonocclusive VAs, whereas 41.9% of patients with MV <18 cm/s also had nonocclusive VAs. Therefore, the criteria of threshold of MV <18 cm/s alone were insufficient to accurately distinguish the After group from the Control group. Using the combination of both MV-ratio ≥1.4 and MV <18 cm/s, sensitivity, specificity, accuracy, and positive predictive value to distinguish the After and PICA end groups from the Control group were much better at 85.2%, 97.4%, 95.9%, and 82.1%, respectively.

The VA blood flow wave and velocity between the After and PICA end groups were similar. Thus, we were unable to distinguish these groups by blood flow alone. Most hypoplastic VAs end in the PICA, and hypoplastic VA has been defined as a VA diameter of <2 mm.[13,23–25] In the present study, the mean and range of VA diameter in the PICA end group were certainly small, at 2.62±0.39 mm and 1.70 to 3.14 mm, respectively, and the PICA end group diameter was the smallest among the 5 groups. Therefore, the hypoplastic VA criteria of <2 mm may be high in specificity but low in sensitivity. When we used a cut-off value of 2.8 mm obtained from sensitivity and specificity curve analysis to distinguish the PICA end group from the After group, the accuracy was 77.8%, which was not overly useful. However, when we used a diameter-ratio ≥1.4 for the analysis, the sensitivity, specificity, and accuracy increased to 93.3%, 91.7%, and 92.6%, respectively, which was superior to that obtained using a cut-off VA diameter value of 2.8 mm. Therefore, a diameter-ratio ≥1.4 was identified as the criterion with which to differentiate between the After and PICA end groups. Diameter-ratio of symptomatic VAs occlusion was usually <1.4. In this study, however, we had 1 symptomatic VA occlusion with the diameter-ratio ≥1.4, which was diagnosed as PICA end by ultrasonography. This point may be one of the limitations in the present study.

Nicolau et al[13] examined RI in VA occlusion but did not discriminate the site of VA occlusion between before and after branching into the PICA. They reported that the RI in VA occlusion was higher than in non-VA occlusion. In the present study, although RI was higher in the After group than in the other groups, MV was superior to RI as a parameter to determine VA occlusion.

In the present study, the MV in 15 (18 vessels) of 117 patients in the Control group was <18 cm/s. Of these 15, 3 had an occlusion at the top of the basilar artery (BA), and 3 had bilateral fetal type of the posterior cerebral arteries (PCA). The blood flow of the VAs may be decreased under such conditions. This finding represents a limitation to the use of our criteria for identification of VA occlusion site.

We did not have any stenotic VAs in our present study. When the origin of VAs had stenosis, the blood flow velocity sometime reduces. Bray et al[26] reported that the velocity curve of severe stenotic VAs with their origin showed isolated ascending and lengthened systolic time and a systolic notch. Therefore, we should be able to distinguish it from the distal VA occlusion.

Another limitation is that asymptomatic acquired VA occlusion cannot always be distinguished from naturally hypoplastic VA ending in the PICA, as differentiating them is difficult in some patients, even with the findings of IA-DSA, MRI, and clinical symptoms. Therefore, the PICA end group may include asymptomatic acquired VA occlusion. In addition, in the present study, there were no patients with bilateral VA occlusion after branching into the PICA. Such patients may have been erroneously assigned into the Control group, because the MV-ratio in patients with bilateral VA occlusion would have been <1.4. Therefore, if a patient's neurological findings suggest occlusive lesions of the BA or VA after branching into the PICA, and the MV of both VAs is <18 cm/s and the MV-ratio is <1.4, those vessels would need to be assessed by transcranial Doppler or transcranial color-coded sonography.

In conclusion, measurement of the blood flow velocity and diameter of the VAs using duplex color-coded ultrasonography can help diagnose the site of VA occlusion. Ultrasonography is a noninvasive tool and can be performed bedside immediately after stroke patient admission. The present VA occlusion criteria may be used to evaluate VA occlusive lesions in acute stroke patients, in particular, those with medullary and brain stem infarction.

References

1. Moneta GL, Edwards JM, Chitwood RW, Taylor LM Jr, Lee RW, Cummings CA, Porter JM. Correlation of North Am Symptomatic Carotid Endarterectomy Trial (NASCET) angiographic definition of 70% to 99% internal carotid artery stenosis with duplex scanning. *J Vasc Surg.* 1993;17:152–159.
2. Kimura K, Yasaka M, Minematsu K, Wada K, Uchino M, Yonemura K, Ogata J, Yamaguchi T. Oscillating thromboemboli within the extracranial internal carotid artery demonstrated by ultrasonography in patients with acute cardioembolic stroke. *Ultrasound Med Biol.* 1998;24:1121–1124.
3. Kimura K, Yonemura K, Terasaki T, Hashimoto Y, Uchino M. Duplex carotid sonography in distinguishing acute unilateral atherothrombotic from cardioembolic carotid artery occlusion. *AJNR Am J Neuroradiol.* 1997;18:1447–1452.

4. Wada K, Kimura K, Minematsu K, Yasaka M, Uchino M, Yamaguchi T. Combined carotid and transcranial color-coded sonography in acute ischemic stroke. *Eur J Ultrasound.* 2002;15:101–108.
5. Yasaka M, Omae T, Tsuchiya T, Yamaguchi T. Ultrasonic evaluation of the site of carotid axis occlusion in patients with acute cardioembolic stroke. *Stroke.* 1992;23:420–422.
6. Wolverson MK, Heiberg E, Sundaram M, Tantanasirviongse S, Shields JB. Carotid atherosclerosis: high-resolution real-time sonography correlated with angiography. *AJR Am J Roentgenol.* 1983;140:355–361.
7. Trattnig S, Hubsch P, Schuster H, Polzleitner D. Color-coded Doppler imaging of normal vertebral arteries. *Stroke.* 1990;21:1222–1225.
8. Trattnig S, Schwaighofer B, Hubsch P, Schwarz M, Kainberger F. Color-coded Doppler sonography of vertebral arteries. *J Ultrasound Med.* 1991;10:221–226.
9. Bendick PJ, Jackson VP. Evaluation of the vertebral arteries with duplex sonography. *J Vasc Surg.* 1986;3:523–530.
10. Bartels E, Fuchs HH, Flugel KA. Duplex ultrasonography of vertebral arteries: examination, technique, normal values, and clinical applications. *Angiology.* 1992;43:169–180.
11. Davis PC, Nilsen B, Braun IF, Hoffman JC Jr. A prospective comparison of duplex sonography vs angiography of the vertebral arteries. *AJNR Am J Neuroradiol.* 1986;7:1059–1064.
12. Kimura K, Yamaguchi T, Yasaka M, Tsuchiya T. [Hemodynamics of the vertebral artery in subclavian steal syndrome and subclavian steal phenomenon]. *Rinsho Shinkeigaku.* 1991;31:970–973.
13. Nicolau C, Gilabert R, Chamorro A, Vazquez F, Bargallo N, Bru C. Doppler sonography of the intertransverse segment of the vertebral artery. *J Ultrasound Med.* 2000;19:47–53.
14. Kimura K, Yasaka M, Moriyasu H, Tsuchiya T, Yamaguchi T. Ultrasonographic evaluation of vertebral artery to detect vertebrobasilar axis occlusion. *Stroke.* 1994;25:1006–1009.
15. Hennerici M, Klemm C, Rautenberg W. The subclavian steal phenomenon: a common vascular disorder with rare neurologic deficits. *Neurology.* 1988;38:669–673.
16. Yip PK, Liu HM, Hwang BS, Chen RC. Subclavian steal phenomenon: a correlation between duplex sonographic and angiographic findings. *Neuroradiology.* 1992;34:279–282.
17. Kliewer MA, Hertzberg BS, Kim DH, Bowie JD, Courneya DL, Carroll BA. Vertebral artery Doppler waveform changes indicating subclavian steal physiology. *AJR Am J Roentgenol.* 2000;174:815–819.
18. Touboul PJ, Mas JL, Bousser MG, Laplane D. Duplex scanning in extracranial vertebral artery dissection. *Stroke.* 1988;19:116–121.
19. Bartels E, Flugel KA. Evaluation of extracranial vertebral artery dissection with duplex color-flow imaging. *Stroke.* 1996;27:290–295.
20. Hoffmann M, Sacco RL, Chan S, Mohr JP. Noninvasive detection of vertebral artery dissection. *Stroke.* 1993;24:815–819.
21. Sturzenegger M, Mattle HP, Rivoir A, Rihs F, Schmid C. Ultrasound findings in spontaneous extracranial vertebral artery dissection. *Stroke.* 1993;24:1910–1921.
22. Osborn AG. The vertebrobasilar system. In: Osborn AG, ed. *Cerebral angiography.* 2nd ed. Philadelphia: Lippincott Williams &Wilkins; 1999: 173–194.
23. Delcker A, Diener HC. [Various ultrasound methods for studying the vertebral artery—a comparative evaluation]. *Ultraschall Med.* 1992;13: 213–220.
24. Tegeler CH, Babikian VL, Gomez CR. Vertebral sonography. *Neurosonology.* 1996;91–92.
25. Fisher CM, Gore I, Okabe N, White PD. Atherosclerosis of the carotid and vertebral arteries—extracranial and intracranial. *J Neuropathol Exp Neurol.* 1965;24:455–476.
26. de Bray JM, Pasco A, Tranquart F, Papon X, Alecu C, Giraudeau B, Dubas F, Emile J. Accuracy of color-Doppler in the quantification of proximal vertebral artery stenoses. *Cerebrovasc Dis.* 2001;11:335–340.

Research article Related Commentary, page 312

Administration of CD34+ cells after stroke enhances neurogenesis via angiogenesis in a mouse model

Akihiko Taguchi,[1] Toshihiro Soma,[2] Hidekazu Tanaka,[3] Takayoshi Kanda,[4] Hiroyuki Nishimura,[5] Hiroo Yoshikawa,[5] Yoshitane Tsukamoto,[6] Hiroyuki Iso,[7] Yoshihiro Fujimori,[8] David M. Stern,[9] Hiroaki Naritomi,[1] and Tomohiro Matsuyama[5]

[1]Department of Cerebrovascular Disease, National Cardiovascular Center, Osaka, Japan. [2]Department of Hematology, Osaka Minami National Hospital, Osaka, Japan. [3]Department of Pharmacology, Graduate School of Medicine, Osaka University, Osaka, Japan. [4]Department of Gynecology, Osaka Minami National Hospital, Osaka, Japan. [5]Department of Internal Medicine, Hyogo College of Medicine, Hyogo, Japan. [6]Department of Pathology, Osaka Medical Center for Cancer and Cardiovascular Disease, Osaka, Japan. [7]Department of Psychology and [8]Department of Hematology, Hyogo College of Medicine, Hyogo, Japan. [9]Medical College of Georgia, Augusta, Georgia, USA.

Thrombo-occlusive cerebrovascular disease resulting in stroke and permanent neuronal loss is an important cause of morbidity and mortality. Because of the unique properties of cerebral vasculature and the limited reparative capability of neuronal tissue, it has been difficult to devise effective neuroprotective therapies in cerebral ischemia. Our results demonstrate that systemic administration of human cord blood–derived CD34+ cells to immunocompromised mice subjected to stroke 48 hours earlier induces neovascularization in the ischemic zone and provides a favorable environment for neuronal regeneration. Endogenous neurogenesis, suppressed by an antiangiogenic agent, is accelerated as a result of enhanced migration of neuronal progenitor cells to the damaged area, followed by their maturation and functional recovery. Our data suggest an essential role for CD34+ cells in promoting directly or indirectly an environment conducive to neovascularization of ischemic brain so that neuronal regeneration can proceed.

Introduction

Thrombo-occlusive atherosclerotic cardiovascular disease is a major cause of death and disability in developed countries. In the acute phase, therapeutic maneuvers include fibrinolytic therapy to restore blood flow to the ischemic site. In the longer term, formation of new blood vessels is necessary to fully supply tissue metabolic and functional requirements. Although it had been assumed that postnatal development of neovessels resulted only from outgrowth of pre-existing vasculature, it has become evident that circulating endothelial progenitor cells (EPCs), contained in a CD34+ cell population enriched in cord blood, have the capacity to participate in neovascularization of ischemic tissues (1, 2). Thus, a new strategy proposed for enhancing recovery due to ischemic stress is administration of EPCs to stimulate formation of neovasculature. In this context, recent reports have demonstrated that infusion of EPCs results in their incorporation into neovasculature at the ischemic site and limitation of tissue damage in animal models (3). Furthermore, human CD34+ cells were shown to secrete numerous angiogenic factors, including VEGF, HGF, and IGF-1 (4). On the basis of these observations, clinical trials of cell transplantation in hindlimb (5, 6) and cardiac ischemia (7) have been initiated with promising results.

Stroke is another setting of occlusive thromboatherosclerotic disease in which acceleration of angiogenesis might be expected to enhance the outcome. Despite the improvement of poststroke neurological outcome by administration of human cord blood cells (8) or bone marrow–derived cells (9) (both potentially a rich sources of stem cells including CD34+ cells) in rodent models, few of the administered cells could be demonstrated in brain parenchyma expressing neuronal markers, raising a question as to the underlying mechanism. The results of our study demonstrate that systemic administration of human CD34+ cells to immunocompromised mice subjected to stroke 48 hours earlier accelerates neovascularization of the ischemic zone. Such a rich vascular environment, along with generation of other nurturing neuronal mediators by CD34+ cells, such as VEGF, FGF2, and IGF-1 (10–12), enhances subsequent neuronal regeneration; endogenous neurogenesis is accelerated as neuronal progenitors migrate to the damaged area, followed by their maturation and survival when CD34+ cells have stimulated the formation of increased vascular channels. In contrast, in the presence of an antiangiogenic agent, the beneficial effect of CD34+ cells was lost. Our results provide the first direct link between vasculogenesis and neurogenesis in the repair of ischemic brain lesions.

Results

Induction of stroke and proliferation of endothelial cells in situ. A reproducible model of stroke in the middle cerebral artery (MCA) cortex, sparing the striatum, was developed in SCID mice by permanent ligation of the M1 distal portion of the left MCA. Subsequent infusion of carbon black showed strongly decreased staining in the affected area. Nonviability of affected tissue was confirmed by 2,3,5-triphenyltetrazolium (TTC) staining. Values of cortical width index (see Methods section) were highly reproducible (~0.34–0.36)

Nonstandard abbreviations used: anterior cerebral artery (ACA); cerebral blood flow (CBF); chloromethylbenzamido (CM-DiI); doublecortin (DCX); endothelial progenitor cell (EPC); erythropoietin (EPO); fetal liver kinase-1 (Flk-1); high-power field (HPF); middle cerebral artery (MCA); neuronal progenitor cell (NPC); neuron-specific nuclear protein (NeuN); phycoerythrin (PE); polysialylated neuronal cell adhesion molecule (PSA-NCAM); subventricular zone (SVZ); 2,3,5-triphenyltetrazolium (TTC).

Conflict of interest: The authors have declared that no conflict of interest exists.

Citation for this article: *J. Clin. Invest.* 114:330–338 (2004). doi:10.1172/JCI200420622.

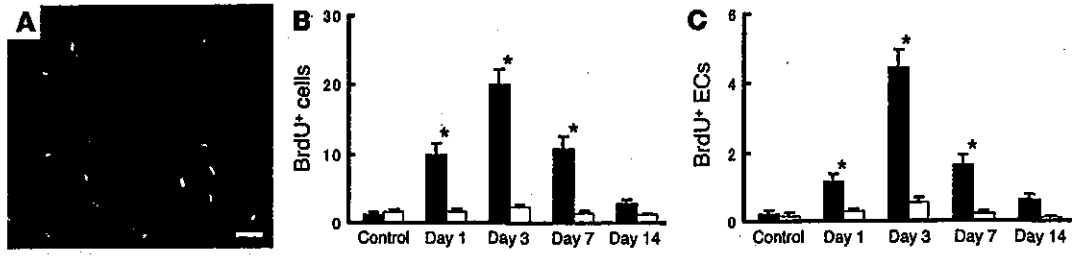

Figure 1

Endothelial proliferation in situ after stroke. On days 1, 3, 7, and 14 after stroke, the number of proliferating cells (BrdU+) and proliferating endothelial cells (co-staining for BrdU and CD31) was determined in the left cortical area of 1–1.5 mm distal from the midline. (**A**) Immunohistological analysis of proliferating cells labeled with BrdU (green), anti-mouse CD31 IgG (red), and both (yellow). The number of cells visualized with BrdU (**B**) and the subpopulation BrdU+ cells also displaying mouse CD31 (i.e., double positives) (**C**) are shown. Ten HPFs were evaluated for each animal ($n = 6$ per group) by two investigators blinded to the experimental protocol. Note in **C**, cells displaying mouse CD31 are termed endothelial cells (ECs). Black bars, ipsilateral; white bars, contralateral. *$P < 0.05$ versus control. Scale bar: 30 μm.

over the 12-week experimental period. Survival in this stroke model was greater than 95%, and no seizures were observed.

To estimate the optimal time to administer human CD34+ cells, proliferation of endothelial cells in vasculature of the penumbral region (at the leading edge of viable tissue) was assessed by in vivo BrdU labeling. Sections were visualized with antibody to BrdU and mouse-specific antibody to CD31 by confocal microscopy. Cellular profiles co-staining for both markers were considered proliferating endothelial cells (Figure 1A). On days 1 and 3 after stroke, a subpopulation of BrdU+ cells also stained with mouse CD31, indicating an endothelial origin of this signal (Figure 1, B and C). By day 7, although endothelial proliferation continued, it had begun to decrease. In contrast, BrdU-labeled cells were present in a constant, small amount on the contralateral (nonstroke) side (Figure 1, B and C). These data indicated that administration of CD34+ cells on day 2 after stroke would buttress the endogenous proliferative component of the vascular response to cerebral ischemia.

Administration of CD34+ cells after stroke. Human CD34+ cells (95% pure CD34+ cells) isolated from human cord blood or control cells (CD34- cells with <0.2% CD34+ cells, also from human cord blood) were administered intravenously via tail vein 48 hours after stroke. Analysis of cell surface markers revealed that 1.5% ± 0.1% and 0.9% ± 0.1% of the CD34+ cell population expressed the endothelial lineage markers fetal liver kinase-1 (Flk-1) (1) and P1H12 (13), respectively ($n = 4$). The effect of CD34+ cells was evident within 24 hours of their transplantation. Labeling vasculature by infusion of carbon black ink demonstrated neovasculature at the border of the MCA and anterior cerebral artery (ACA) cortex (staining with TTC demarcates viable and nonviable tissue) in animals treated with CD34+ cells (Figure 2, A and B), compared with those receiving CD34- cells (Figure 2C) or PBS alone (Figure 2D). Determination of the angiographic score confirmed the impression of increased neovasculature in animals transplanted with CD34+ cells, compared with other groups (Figure 2E). To evaluate vascular activation in affected cerebral vessels, we used mouse-specific antibody to CD13, an antigen expressed by endothelial cells in angiogenic, but not quiescent, vasculature (14). Visualization of mouse CD13 in brain sections 24 hours after cell transplantation showed that cells bearing this activated endothelial marker were most evident in sections from mice treated with CD34+ (Figure 2F), compared with those receiving CD34- cells (Figure 2G) or PBS (Figure 2H). Increased density of vasculature in the ischemic territory of animals treated with CD34+ cells translated to significantly enhanced cerebral blood flow (CBF) (Figure 2I).

To analyze the effect of subpopulations within the general CD34+ cell population, we compared the effect of poststroke transplantation of the same number of CD34+ cells (containing Flk-1- and Flk-1+ cells) with CD34+/Flk-1- cells on vascular activation and neovascularization. Brain tissue was examined 7 days after cell transplantation, because EPCs are known to incorporate into capillary walls at ischemic sites by this time point after the ischemic episode (2). FACS analysis confirmed that the CD34+/Flk-1- population contained less than 0.1% Flk-1+ cells ($n = 4$). On the basis of CD13 staining (using the same mouse-specific antibody mentioned earlier), there was similar activation of endogenous endothelium after transplantation of either CD34+ cells (including both Flk-1- and Flk-1+ subpopulations) and CD34+/Flk-1- cells (not shown). Although neovasculature was observed at the border of the MCA and ACA cortex in animals treated with CD34+ cells (Figure 2J) and CD34+/Flk-1- cells (Figure 2K), mice treated with CD34+ cells displayed increased neovascularization based on angiographic score (scores of 2.2 ± 3 and 1.3 ± 2, for CD34+ and CD34+/Flk-1- cells, respectively; $P < 0.05$, $n = 6$).

Transplantation of CD34+ cells and poststroke functional recovery. Stroke causes motor deficits and behavioral abnormalities (15). Dysfunction of the cortex is closely linked to disinhibition of behavior (16). Compared with sham-operated controls, mice that received CD34- cells or PBS displayed significant behavioral abnormalities on day 90 after cell transplantation ($n = 12$, for each group). Rearing counts under lighted conditions were 8.4 ± 0.8 (PBS), 8.7 ± 0.5 (CD34- cells), 4.2 ± 0.5 (CD34+ cells), and 3.0 ± 0.5 (sham-operated controls) for each of the groups. Counts of locomotion were 5.1 ± 0.4 (PBS), 5.0 ± 0.4 (CD34- cells), 3.7 ± 0.4 (CD34+ cells), and 3.3 ± 0.4 (sham). ANOVA revealed hyperactivity with respect to both rearing ($P < 0.01$) and locomotion ($P < 0.01$) in the CD34- cell– and PBS-treated groups, compared with sham-operated controls. In contrast, mice treated with CD34+ cells showed no significant hyperactivity compared with sham-operated controls ($P > 0.05$), and displayed significant improvement in both behavioral tests compared with animals that received PBS or CD34- cells ($P < 0.05$). Mice treated with CD34- cells or PBS after stroke showed loss of this "dark" response, with respect to rearing ($P > 0.05$) and locomotion ($P > 0.05$). In contrast, animals treated with CD34+ cells displayed the expected increase in rearing and locomotion in the darkness ($P < 0.01$).

Using another behavioral paradigm, excessive startle consequent to auditory stimulation was observed in poststroke animals treated with CD34- cells and PBS. Startle amplitudes were 0.9 ± 0.1 volts (PBS), 0.8 ± 0.1 (CD34- cells), 0.5 ± 0.1 (CD34+

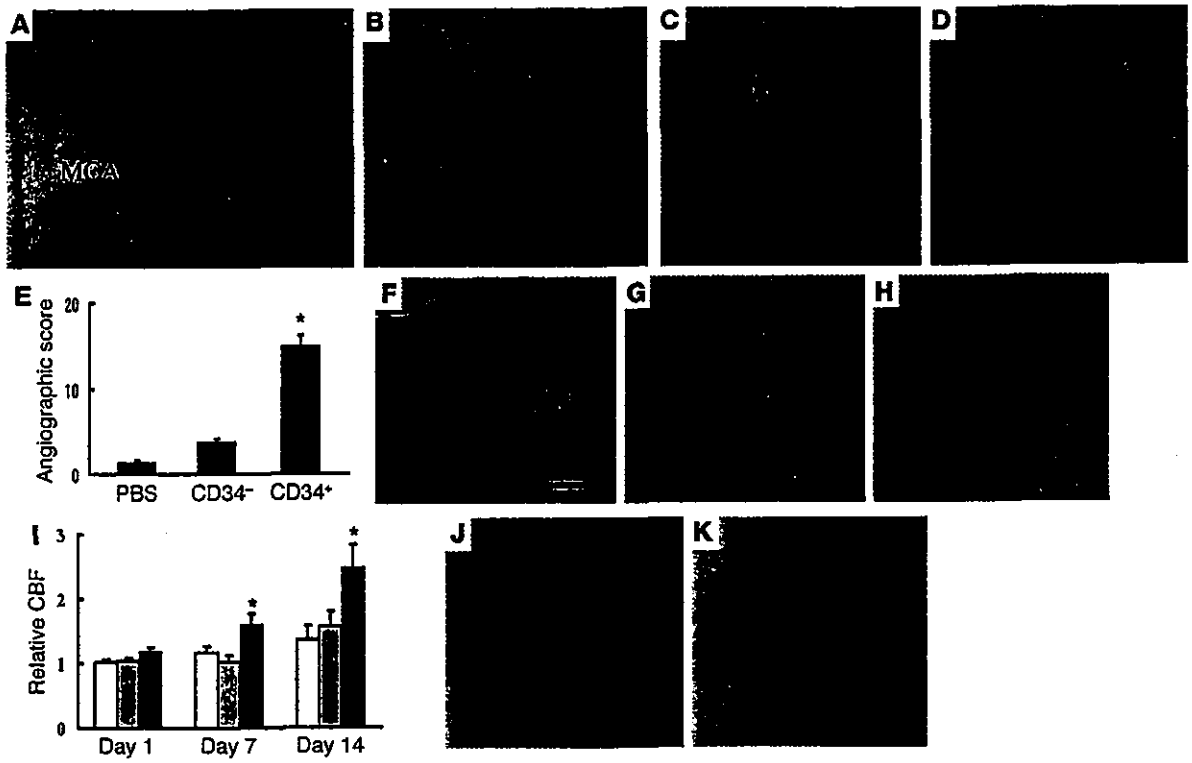

Figure 2

Transplantation of CD34⁺ cells after stroke accelerates neovascularization. (**A–D**) Mice subjected to stroke received CD34⁺ cells (**A** and **B**), CD34⁻ cells (**C**), or PBS alone (**D**) on day 2. Animals were infused with carbon black ink and killed at 24 hours after cell transplantations. Sections were stained with TTC. Neovascularization was noted at the border zone between the ACA and MCA areas (arrowheads show microvessels), especially in animals treated with CD34⁺ cells compared with those receiving CD34⁻ cells or PBS alone. (**E**) An angiographic score for each experimental condition based on analysis of 6 mice per group. (**F–H**) Activated endothelial cells were observed with antibody specific for mouse CD13 in the ACA area. **F**: CD34⁺ cells; **G**: CD34⁻ cells; **H**: PBS. (**I**) CBF was measured in the MCA area just outside of the penumbra, and values in animals treated with CD34⁺ cells (black bars), CD34⁻ cells (gray bars), or PBS (white bars) were compared with values before cell transplantation at times corresponding to days 1, 7, and 14 after cell transplantation ($n = 6$ per group). Data shown are relative CBF versus day the measurement was performed. (**J** and **K**) Labeling vasculature by infusion of carbon black ink demonstrated neovasculature at the border of the MCA and ACA cortex in animals treated with CD34⁺ cells (**J**) and CD34⁺/Flk-1⁻ cells (**K**) on day 7 after cell transplantation. Scale bars: 0.5 mm (**A**) and 0.1 mm (**B**, **F**, and **J**). *$P < 0.05$ versus PBS.

cells), and 0.4 ± 0.1 (sham) on day 90. ANOVA revealed hyperactivity in the CD34⁻ cell– and PBS-treated groups, compared with sham-operated controls ($P < 0.05$). In contrast, mice treated with CD34⁺ cells showed no significant hyperactivity compared with sham-operated controls ($P > 0.05$). Shortening of the latency period with fear conditioning was also observed in poststroke animals treated with CD34⁻ cells and PBS compared with sham-operated controls ($P < 0.05$). In contrast, mice treated with CD34⁺ cells showed no significant hyperactivity ($P > 0.05$). Similar behavioral abnormalities were also observed on day 35 after cell transplantation. Since ischemic injury in our stroke model was limited to the cortex (hippocampus and striatum were intact), it was not surprising that spatial learning (water maze testing) and passive avoidance remained unchanged and comparable in all groups when assessed 5 weeks after stroke (data not shown). Mice showed rapid recovery from focal motor deficits, and by day 16 after stroke no motor deficits were detected using a modified three-point scale (17) (data not shown).

Effect of poststroke CD34⁺ cell transplantation on endogenous neurogenesis and cortical expansion. These results suggested that cortical function and neoangiogenesis, potentially supporting integrity of the MCA cortex, might be better maintained in animals treated with CD34⁺ cells after stroke. Such maintenance of cortical integrity might reflect CD34⁺ cell–mediated enhancement of the survival of ischemic neurons or acceleration of endogenous neurogenesis. Representative brains from poststroke animals in each group (treated with PBS alone, CD34⁻ cells, or CD34⁺ cells) are shown in Figure 3, A–F. There was a prominent increase in cortical width index in animals receiving CD34⁺ cells at 14, 35, and 90 days after cell transplantation (Figure 3G). Thus, cortical expansion in animals treated with CD34⁺ cells was most likely to reflect the result of ongoing neurogenesis, rather than maintenance of the integrity of ischemic neurons from the time of induction of stroke.

Cell trace analysis with a fluorescent dye revealed that labeled transplanted CD34⁺ cells were not co-stained with antibody to a neuronal (neuron-specific nuclear protein; NeuN) or an astrocyte (glial fibrillary acidic protein) marker (not shown). However, activation of endogenous neurogenesis was observed after stroke, and this was accentuated in mice receiving CD34⁺ cells. On day 7 after administration of CD34⁺ cells, cells expressing the polysialylated neuronal cell adhesion molecule (PSA-NCAM), a marker of migrating neuronal progenitor cells (NPCs) (18), were observed in the subventricular zone (SVZ), and migration of these NPCs toward the ischemic zone was visualized on day 14 using markers

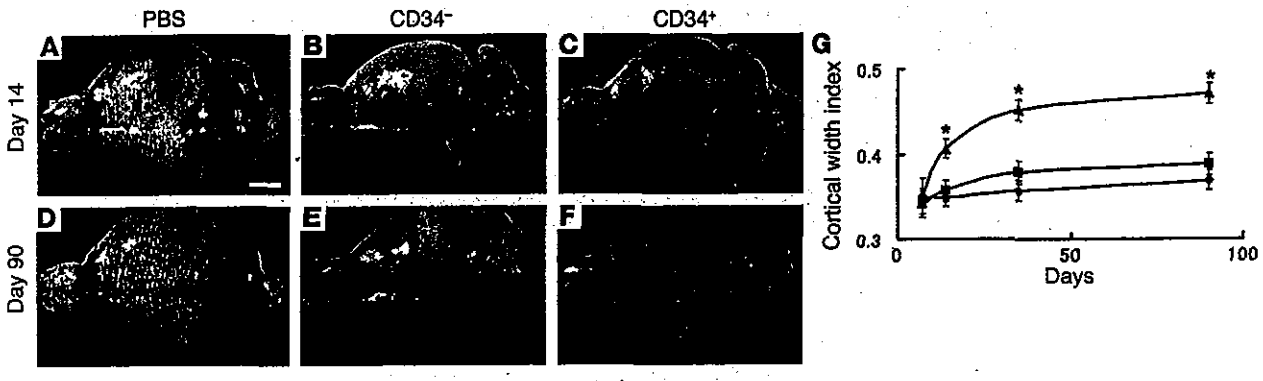

Figure 3
CD34⁺ cell transplantation induces cortical expansion after stroke. (**A–F**) On day 14 (**A–C**), and day 90 (**D–F**) after cell transplantation, the brains of mice were evaluated grossly. Compared with poststroke mice treated with PBS (**A** and **D**) or infused with CD34⁻ cells (**B** and **E**), animals transplanted with CD34⁺ cells (**C** and **F**) showed an increase in area occupied by the left cortex. (**G**) Cortical regeneration was induced by CD34⁺ cells transplantation: triangles, CD34⁺ cells; squares, CD34⁻ cells; diamonds, PBS. In each case, there were 6 animals per group. Scale bar: 2 mm (**A**). *$P < 0.05$ versus PBS.

for PSA-NCAM (Figure 4, A and B, corresponding to lower and higher magnifications, respectively), as well as the neuronal stem cell marker, Musashi-1 (Figure 4C) (19). Expression of doublecortin (DCX), a marker of immature, or early, neurons (20), was principally restricted to NPCs close to the SVZ (Figure 4D). In contrast, expression of a neuronal cell marker, NeuN, was observed after cell migration from the SVZ and appeared as a signal of lower intensity compared with nearby mature neurons (Figure 4E). The situation was quite different on the contralateral side in poststroke animals treated with CD34⁺ cells; no such movement of precursors (PSA-NCAM⁺ cells) was observed (Figure 4F). Although migrating NPCs were also seen in poststroke animals treated with PBS (Figure 4G) and CD34⁻ cells, this finding was considerably magnified in mice receiving CD34⁺ cells (Figure 4H).

To investigate mechanisms underlying cortical expansion, immunohistological analysis was conducted to visualize PSA-NCAM, NeuN, and MAP-2. On day 14 after transplantation of CD34⁻ cells after stroke, mature cortical neurons displaying neuronal markers NeuN (Figure 5A) and MAP-2 (Figure 5B) were observed up to the periphery of the ischemic area, whereas only a thin layer of migrating PSA-NCAM⁺ NPCs was observed at the ischemic edge (Figure 5C). In contrast, transplantation of CD34⁺ cells after stroke expanded cortical areas displaying a low density of NeuN⁺ (Figure 5D) and MAP-2⁺ cells (Figure 5E) beyond the boundary demarcating mature neurons. Migration of NPCs into this expanded area was also observed by PSA-NCAM staining (Figure 5F).

Next, we investigated the fate of NPCs migrating from the SVZ to the ischemic area. Poststroke animals treated with CD34⁻ cells displayed many cells with TUNEL⁺ nuclei around the lower part of cortical ischemic edge (Figure 5G). In contrast, there were a minimal number of TUNEL⁺ nuclei observed in the same region in animals subject to transplantation of CD34⁺ cells after stroke (Figure 5, H and I). Thus, animals treated with CD34⁺ cells after stroke display migration and survival of NPCs, which eventually contribute to a population of more mature neurons.

To confirm this evidence of neurogenesis, animals transplanted with CD34⁺ cells, CD34⁻ cells, or PBS after stroke were infused with

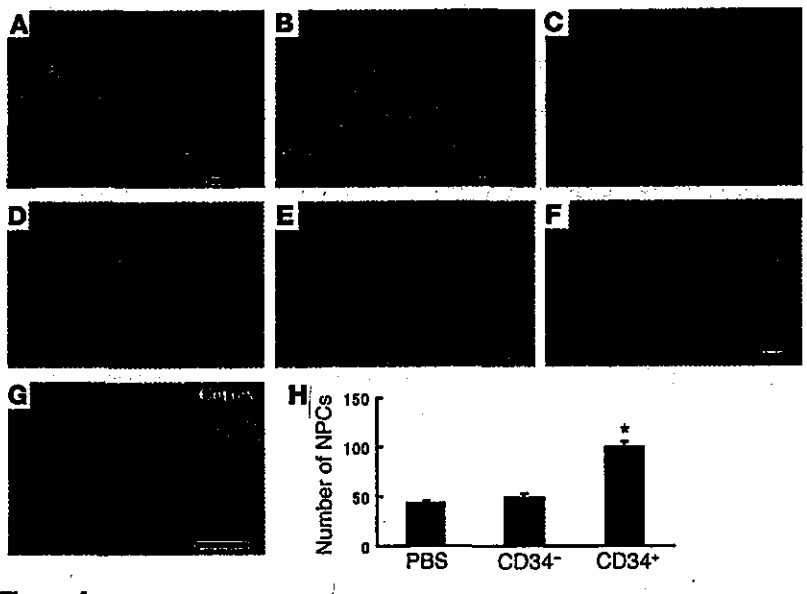

Figure 4
CD34⁺ cell transplantation accelerates neuronal regeneration after stroke. (**A** and **B**) On day 14, animals receiving CD34⁺ cells after stroke displayed migration of NPCs toward the ischemic area by PSA-NCAM immunostaining. (**C–E**) Analysis of serial sections displayed expression of neuronal stem cell markers, Musashi-1 (**C**) and DCX (**D**). Note that expression of DCX was limited to the area proximal to the SVZ. PSA-NCAM⁺ NPCs also expressed NeuN (**E**). Small NeuN⁺ nuclei were observed in PSA-NCAM⁺ NPCs, whereas more intensely staining and larger nuclei represent mature neurons. (**F**) On day 14 on the contralateral side, PSA-NCAM⁺ NPCs were limited to the SVZ; that is, no migration of NPCs was observed. (**G**) Migration of NPCs with small NeuN⁺ nuclei toward cortex was observed in poststroke mice treated with PBS on day 14 after cell transplantation. (**H**) The average number of NPCs in the white matter at the lower left of the left cortex per HPF from 5 animals under each condition. Three sections were evaluated in each animal, and $n = 5$ per group. Arrowheads delineate individual NPCs or demarcate areas rich in NPCs. Scale bars: 1 mm (**A**), 0.2 mm (**B** and **F**), and 0.4 mm (**G**). *$P < 0.05$ versus PBS.

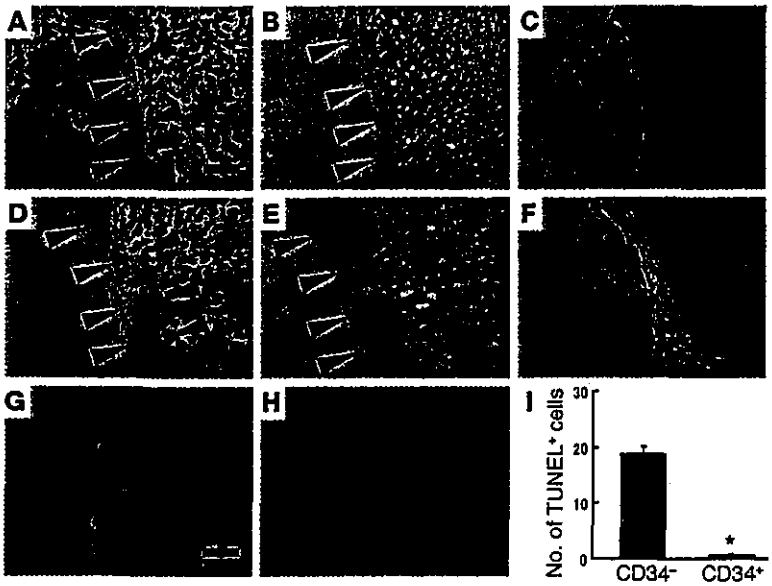

Figure 5
Therapeutic neovascularization, due to CD34+ cell transplantation after stroke, enhances neurogenesis. (**A–F**) On day 14 after CD34- cell transplantation, mature cortical neurons were observed up to the edge of the ischemic region displaying neuronal markers, NeuN (**A**) and MAP-2 (**B**), whereas only a thin layer of migrating PSA-NCAM+ NPCs was observed at the ischemic edge (**C**). In contrast, after transplantation of CD34+ cells, expanded cortical areas displaying a low density of NeuN+ (**D**) and MAP-2+ cells (**E**) were observed beyond the boundary demarcating mature neurons. Migration of NPCs into this expanded area was also observed by PSA-NCAM staining (**F**). (**G–I**) On day 14, TUNEL+ cells were visualized around the lower part of the expanded cortical area. Whereas massive cell death was observed in animals receiving CD34- cell transplantation (**G**), the number of TUNEL+ profiles was strongly reduced in mice transplanted with CD34+ cells (**H**). (**I**) The average number of TUNEL+ cells per HPF. Three sections were evaluated in each animal; $n = 5$ per group. Arrowheads indicate the expanded cortical areas displaying a low density of indicated marker. Scale bars: 100 μm (**A**) and 50 μm (**G**). *$P < 0.05$ for CD34+ versus CD34- cell transplantation.

BrdU every second day for a total of 14 days and then killed. BrdU- and NeuN-bearing cell populations were visualized to determine if a group of neurons might be undergoing cell division. In animals treated with PBS alone (Figure 6A) or CD34- cells (Figure 6B), double staining for BrdU and NeuN displayed little evidence of cells (i.e., nuclei) expressing both markers. Only in animals infused with CD34+ cells after stroke did we consistently observe double-labeled cell profiles with BrdU and NeuN to produce a merged image with cells displaying both markers (Figure 6C). Quantification of these results showed a significant increase in double-positive profiles (i.e., cells co-staining with antibody to BrdU and NeuN) in poststroke animals infused with CD34+ cells (Figure 6D). Consistent with these data, total neuronal counts (Figure 6E) from sections stained with NeuN in the left cortex 90 days after cell transplantation demonstrated a significant increase in the number of cells visualized in animals transplanted with CD34+ cells compared with those receiving CD34- cells or PBS. In addition, vasculature was visualized in the ischemic zone of the forebrain of animals treated with CD34+ cells 90 days later using anti-mouse CD31 as a marker. A distinct vascular network was seen in the expanded cortex associated with neurogenesis after stroke (Figure 6F). Such vessels displayed a pattern quite distinct from that observed on the contralateral (nonischemic) side (Figure 6G). In these vessels on the ischemic side, some endothelial cells were observed to express human CD31 antigen (Figure 6H). On day 90, mature MAP-2+ dendrites were observed *in* the expanded cortex of poststroke animals treated with CD34+ cells (data not shown). These data are consistent with the formation of a stable neovasculature to support regeneration of cortical neurons.

Inhibition and acceleration of angiogenesis by antiangiogenic and angiogenic agents. To investigate the hypothesis that neovascularization is essential to support endogenous neuronal regeneration, we used an antiangiogenic agent, Endostatin. The latter is known to inhibit proliferation of endothelial cells (21) and to have a direct inhibitory effect on EPCs (22). Mice were subjected to stroke, CD34+ or CD34- cells were administered, and animals were divided into two groups; one group received Endostatin and the other PBS ($n = 5$, for each group). On day 7 after cell transplantation, treatment with Endostatin suppressed endothelial proliferation to 18% ± 3% and 22% ± 3% in mice transplanted with CD34- cells and CD34+ cells, respectively, compared with proliferation observed in PBS-treated controls. Administration of Endostatin also impaired cortical expansion due to transplantation of CD34+ cells. On day 14, the cortical width index was 0.33 ± 0.01 and 0.41 ± 0.01 with and without Endostatin, respectively ($P < 0.01$). Animals treated with CD34+ cells and Endostatin after stroke displayed a reduction in migrating NPCs; 101 ± 7 cells per high-power field (HPF), for animals treated with CD34+ cells + PBS, and 21 ± 2 cells/HPF for animals treated with CD34+ cells + Endostatin ($P < 0.01$). Similarly, on day 14, the number of neurons in the poststroke cortex was less in mice treated with CD34+ cells + Endostatin (1,469 ± 53), compared with animals treated with CD34+ cells + PBS (2,213 ± 36; $P < 0.01$).

To gain further support for our hypothesis, we used the proangiogenic agent erythropoietin (EPO). EPO, well known for its essential role in regulating proliferation and differentiation of erythroid cells, has recently been found to promote mobilization of EPCs (23) and to have angiogenic potential (24). On day 4 after stroke, a significant increase in circulating CD34+ cells was observed with EPO injection (5,244 ± 1,267 and 1,333 ± 389 cells/ml in the EPO and PBS groups, respectively; $n = 6$ per group, $P < 0.05$). In addition, mice treated with EPO displayed enhanced neovascularization based on angiographic score (5.4 ± 0.8 and 1.2 ± 0.4, in EPO and PBS groups, respectively; $n = 5$ per group, $P < 0.05$). On day 28 after stroke, treatment with EPO increased the number of cells co-staining for BrdU and NeuN (3.4 ± 0.3 and 0.4 ±0.1/HPF in the EPO and PBS groups, respectively; $n = 5$ per group, $P < 0.05$). It should be noted that the magnitude of the stimulatory effect of EPO treatment on angiogenesis and neurogenesis in these experiments was less than that observed in studies with CD34+ cell transplantation, probably because of the greater number of cells transferred in the latter case.

Neurogenesis in 24-week-old mice. To analyze the effect of increased age on accelerated neurogenesis associated with CD34+ cell transplantation, 24-week-old SCID mice were used. Compared with poststroke mice treated with CD34- cells (Figure 7A), transplantation of CD34+ cells (Figure 7B) showed a significant increase in area occupied by the left cortex on day 35 (Figure 7C). In addi-

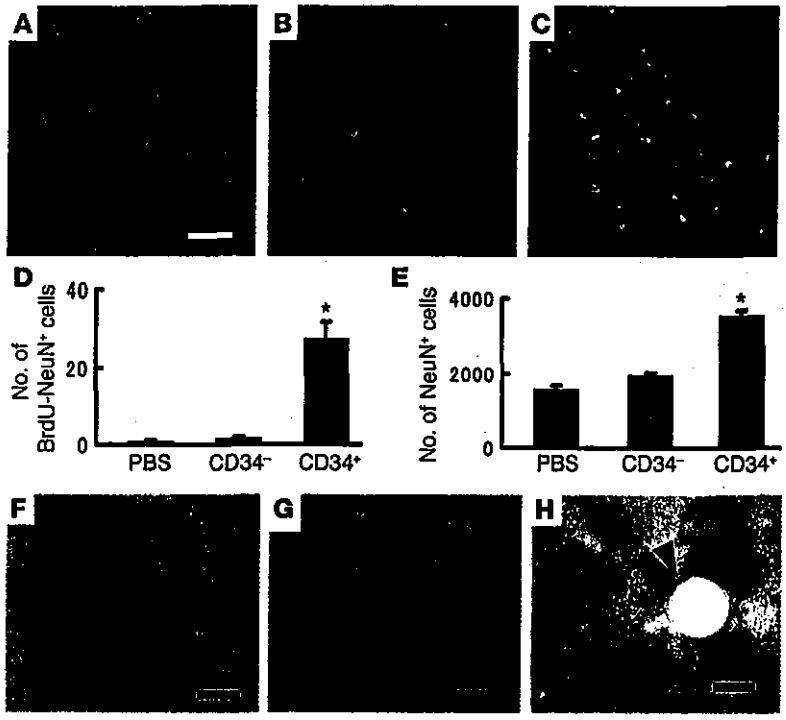

Figure 6
Therapeutic neovascularization supports survival of regenerating neurons. (**A–C**) Animals treated with PBS alone (**A**), CD34⁻ cells (**B**), or CD34⁺ cells (**C**) were infused with BrdU, killed, and studied immunohistochemically with antibody to BrdU (red), NeuN (green), or both (yellow). (**D**) The average number of double-positive cells (stained with antibody to BrdU and NeuN) per HPF on day 90 after cell transplantation. Ten fields were evaluated in each animal, and $n = 6$ per group. $^*P < 0.05$ versus PBS. (**E**) On day 90 after cell transplantation, brain sections from animals treated with PBS alone, CD34⁻ cells, or CD34⁺ cells were stained with antibody to NeuN, and the number of total neurons in the left cortex was counted. (**E**) The average number of total NeuN⁺ cells in the left cortex. $n = 6$ per group; $^*P < 0.05$ versus PBS. (**F** and **G**) On day 90 after cell transplantation, mouse CD31 was visualized immunohistologically in forebrain sections from poststroke animals. Newly formed vascular networks were observed in the expanded cortex. The vascular pattern displayed by these neovessels on the ipsilateral (**F**, ischemic side) was different from that observed on the contralateral side (**G**). (**H**) On day 90, human CD31 was visualized immunohistologically. Human endothelial cells were observed in the regenerating cortex of animals treated with CD34⁺ cells after stroke. The arrowhead shows a human CD31⁺ endothelial cell. Scale bars: 50 μm (**A**), 100 μm (**F** and **G**), and 20 μm (**H**).

tion, evidence of vascular activation, as judged by reactivity with anti-CD13 antibody, was observed in mice treated with CD34⁺ cells (Figure 7D, CD34⁻ cells; Figure 7E, CD34⁺ cells). Migration of NPCs was observed in mice treated with CD34⁻ cells (Figure 7F) and CD34⁺ cells (Figure 7G), but a significant enhancement was observed in animals receiving CD34⁺ cells (Figure 7H). Only a thin layer of migrating PSA-NCAM⁺ NPCs was observed at the ischemic edge in animals treated with CD34⁻ cells (Figure 7I). In contrast, CD34⁺ cell transplantation resulted in a much thicker layer of PSA-NCAM⁺ cells (Figure 7J). Comparing these data in 24-week-old animals with our previous results using 5-week-old mice, the older animals displayed a similar cortical width index (5 weeks old, 0.45 ± 0.01; 24 weeks old, 0.43 ± 0.02; $P > 0.05$), although older age was associated with a decrease in NPCs migrating into the cortex (5 weeks old, 71 ± 3 cells/HPF; 24 weeks old, 43 ± 4 cells/HPF; $P < 0.05$) on day 35 after CD34⁺ cell transplantation.

Discussion

Our findings show that administration of human CD34⁺ cells to immunocompromised mice 48 hours after stroke enhances neovascularization at the border of the ischemic zone followed by endogenous neurogenesis. Furthermore, suppression of the neo-

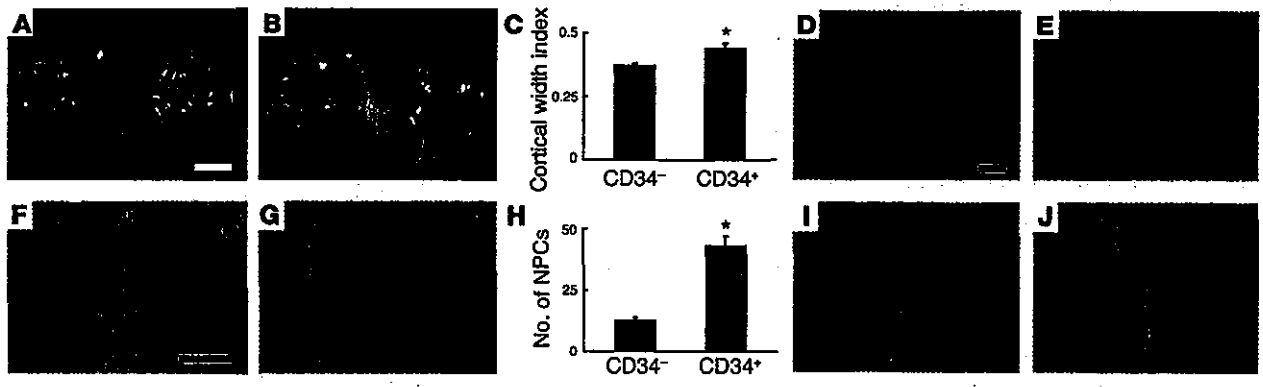

Figure 7
CD34⁺ cell transplantation in 24-week-old animals. (**A–C**) On day 35 after cell transplantation, the brains were evaluated. Compared with poststroke mice treated with CD34⁻ cells (**A**), animals transplanted with CD34⁺ cells (**B**) showed an increase in area occupied by the left cortex. Significant cortical regeneration was induced by CD34⁺ cells transplantation (**C**). (**D** and **E**) Compared with CD34⁻ cell transplantation (**D**), increased evidence of activated vasculature was observed in animals receiving CD34⁺ cells (**E**), as detected with mouse specific anti-CD13 antibody. (**F–H**) Migration of NPCs (small NeuN⁺ nuclei migrating toward the cortex) was observed in poststroke mice treated with CD34⁻ cells (**F**) and with CD34⁺ cells (**G**). However, a significant increase in migrating NPCs was induced by CD34⁺ cell transplantation (**H**). (**I** and **J**) A thin layer of migrating PSA-NCAM⁺ NPCs was observed at the ischemic edge of the cortex in animals treated with CD34⁻ cells (**I**), compared with a much thicker layer in those receiving CD34⁺ cells (**J**). Scale bars: 2 mm (**A**), 0.1 mm (**D** and **I**), and 0.4 mm (**F**). $n = 4$ in each group; $^*P < 0.05$ versus CD34⁻ cells.

vascularization by an antiangiogenic agent impaired neurogenesis. On the basis of these data, accelerated neovessel formation seems to be essential for enhancing endogenous neurogenesis and improving functional recovery.

The generation of new neurons in the adult is largely restricted to two regions: the SVZ lining the lateral ventricles and the subgranular zone of the dentate gyrus (25). In the transient cerebral ischemia model, evidence has been provided that neuronal regeneration occurs (10, 20). However, even in a transient ischemia model in which integrity of the microcirculation is maintained, it was shown that greater than 80% of newly formed neurons died, most likely because of unfavorable environmental conditions including lack of trophic support and exposure to products of damaged tissue. These considerations may underlie the observation that only 0.2% of nonviable ischemic neurons were replaced through neurogenesis (20). Such previous observations are consistent with our current results in animals treated with $CD34^-$ cells or PBS, in which there was no enhancement of neovascularization, no neurogenesis, and no functional recovery.

Consistent with these data, Endostatin-mediated suppression of endothelial proliferation and direct effects on EPCs abrogated the beneficial effect $CD34^+$ cells on neurogenesis and cortical expansion, and at the same time inhibited formation of neovasculature after stroke. In contrast, when EPO was used as a proangiogenic agent (recently, EPO has also been found to promote mobilization of EPCs) (23, 24), accelerated formation of neovasculature was accompanied by enhanced neurogenesis after stroke in our murine model. Our data provide the first direct link between therapeutic neovascularization after stroke and enhanced neurogenesis; formation of neovasculature after stroke supported neurogenesis. Consistent with a previous report (26), activation of NPCs after stroke was induced in adult, as well as young, murine brain. The number of activated NPCs was less in the adult animals, but a significant increase was still observed consequent to $CD34^+$ cells transplantation, with evidence of activated vasculature in brains of the older animals. These findings support our hypothesis that administration of $CD34^+$ cells provides a milieu favorable for neovascularization and endogenous neurogenesis, even in the mature brain.

A relationship between angiogenesis and neurogenesis would be consistent with regeneration of parenchymal cells in other organs subject to therapeutic angiogenesis (27, 28). Mechanisms underlying this observation might include more optimal preparation of the ischemic tissue bed for neuronal regeneration by accelerated removal of debris and toxic products, and/or the enhanced production of chemokines and trophic agents by neovasculature. Factors involved might be FGF2 (11), PDGF (29), brain-derived neurotrophic factor (30), and IL-8 (31), which have the capacity to induce mitogenesis, differentiation, recruitment, and survival of NPCs and newly generated neurons. In addition, mediators produced by $CD34^+$ cells (4), such as VEGF, FGF2, and IGF-1, have been shown to accelerate endogenous neurogenesis (10–12). The effects of these and other factors derived from $CD34^+$ cells (32, 33) acting on the vasculature are also likely to have an important role in providing an environment conducive to neurogenesis. Newly formed neurons in the setting of neovascularization have been shown to integrate into neuronal networks in adult animals (34); in fact, lack of participation of neurons in such neuronal circuits is probably associated with cell death (20). Our results provide strong support for the hypothesis that neovascularization consequent to administration of $CD34^+$ cells induces neurogenesis by providing the necessary supportive environment. Whereas perturbation of the neurovascular unit has been proposed to contribute to tissue damage in stroke, neoangiogenesis and accompanying neurogenesis could be considered to be rebuilding crucial elements of the neurovascular unit (35). Previous reports have demonstrated that endothelial cells in newly formed vessels after stroke mainly originate from pre-existing endothelial cells (due to proliferation) with a contribution of circulating EPCs (36, 37). Consistent with these findings, we observed proliferating mouse endothelial cells around the ischemic area soon after stroke. The latter endothelial cells could be visualized, at least in part, with antibody specific for human CD31, after transplantation of human $CD34^+$ cells. Furthermore, diminished neovascularization was observed after stroke following transplantation of $CD34^+/Flk\text{-}1^-$ cells, compared with $CD34^+$ cells (containing both $Flk\text{-}1^-$ and $Flk\text{-}1^+$ cells) despite similar activation of murine endothelial cells in the ischemic territory in each case. These results support potential contribution of $CD34^+/Flk\text{-}1^+$ cells (a population known to be rich in EPCs) in expansion of the vascular network after stroke.

The actual pattern of the newly formed vascular network was quite different on the ipsilateral (ischemic) from the contralateral side in poststroke mice treated with $CD34^+$ cells. This observation suggests that formation of vasculature consequent to transplantation of $CD34^+$ cells after stroke does not simply reconstitute the original vascular network. Rather, a new vascular pattern arises (a true neovasculature) that is capable of supporting neurogenesis, followed by functional recovery, even though it displays a relatively "aberrant" pattern, at least anatomically, compared with the contralateral vasculature.

Our observations provide evidence of a crucial role for neovessel formation, achieved through the administration of $CD34^+$ cells after stroke, in processes that underlie neurogenesis. These data strongly suggest that neovascularization is essential for neuronal regeneration after stroke and that therapeutic neovascularization is a potentially effective means of enhancing functional recovery. Our observations might explain the mild therapeutic effect achieved by neuronal cell transplantation after stroke reported in humans (38). This leads to the hypothesis that therapeutic neovascularization may be required to achieve optimal "take" of transplanted neuronal precursors in the setting of ischemia. Although the current data bear most directly on the endogenous neuronal response to cerebrovascular ischemia, it is possible that enhanced formation of neovasculature may also be important for survival of embryonic (39) and neural (40) stem cell transplants in other circumstances, such as neurodegenerative disorders.

Methods

All procedures were done in accordance with the National Cardiovascular Center Animal Care and Use, and Human Assurance Committees. Quantitative measurements and behavioral tests were conducted by investigators blinded to the experimental protocol and identity of the sections and animals under study.

Induction of focal cerebral ischemia. Permanent focal cerebral infarction was produced by ligation and disconnection of the distal portion of the left MCA. Male SCID mice (5 weeks old; Oriental Yeast Co. Ltd., Tokyo, Japan) were used for experiments involving human cell transplantation. Male C57BL/6J mice (24 weeks old; Clea Japan Inc., Tokyo, Japan) were used for experiments with human recombinant EPO (Kirin, Tokyo, Japan). Under halothane inhalation (3%), the left MCA was isolated, electrocauterized, and disconnected just distal to its crossing of the olfactory tract (distal M1 portion). CBF in the MCA area was monitored as described (41). Mice that showed decreased CBF by approximately 75% immediately after and 24 hours after ligation were used for our experiments (success rate of >95%). Body temperature was maintained at 36.5–37°C using a heat lamp during